ECOLOGICAL CONTROLS ON SUCCESSIONAL PATTERNS IN BLOOM-FORMING CYANOBACTERIA

A Thesis Presented for the
Master of Science
Degree
The University of Tennessee, Knoxville

Kyla L. Hooker
May 2022

ABSTRACT

Harmful algal blooms are widespread in lake ecosystems but the ecological factors underlying their formation and maintenance are poorly understood. We revisit classical ecological theories which characterize and evaluate contrasting bottom-up and top-down influences on the selection of phytoplankton groups, such as *Microcystis aeruginosa*. We begin with a data compilation and analysis of environmental data from Lake Erie. This data analysis of nutrient concentrations, pigment concentrations, and zooplankton biomasses helps us understand and interpret what is happening in the environment throughout the year. Thus, allowing us to build a mathematical model to test our hypothesis. Our mathematical model asses a community in which two producers compete for a resource, which is supplied at a high constant rate and a consumer which can feed on either producer. Raised nutrient input may enhance selective pressure for defensive groups when high cell densities lead to high contact rates between predators and prey. We report work which evaluates whether these idealized predictions hold in more complex models which account for non-equilibrium influences associated with variable resource supply and temperature. Overall, we hypothesize that increases in resource inflow and temperature increase contact rates between predators and prey, shifting selection pressure toward defense against predation, which may be a major reason why *Microcystis aeruginosa* are selected in hyper-eutrophic lakes.

TABLE OF CONTENTS

LIST OF TABLES

LIST OF FIGURES

CHAPTER ONE: INTRODUCTION AND GENERAL INFORMATION

Eutrophication is a process in which bodies of water receive excess nutrients due to runoff from agricultural lands, animal manure, and factories (Rast & Thornton, 1996). These excess nutrients such as phosphorus and nitrogen cause an overgrowth in plant and algal life (Rast & Thornton, 1996). Some of these seasonal algal blooms can be classified as harmful algal blooms (HABs) due to the release of toxins and contribution to anaerobic conditions (Carmichael, 1994a). HABs of the single-celled cyanobacterium *Microcystis aeruginosa* are increasing in shallow lakes globally (Wilhelm et al., 2020). However, the ecological and environmental contributions to these *Microcystis* blooms are not fully understood. We want to investigate what mechanisms, drivers, and conditions favor the growth of *Microcystis* during the late summer blooms.

Eutrophication

In a healthy ecosystem, nitrogen and phosphorus enter into the water system at a rate that sustains microorganisms without allowing for excessive growth. Microscopic organisms, such as phytoplankton and bacteria, use these critical elements for primary productivity. The health of these microscopic communities is essential because they are the base of nearly all aquatic food-webs allowing for the healthy growth at higher trophic levels (Ebert et al., 2001). Predators such as microzooplankton grazers and viruses consume the photosynthetic microbes, which keeps the population size in check and allows for

clear waters. Thus, sunlight can penetrate through the water column and give other photosynthetic plants the energy needed for photosynthesis**.** As more agricultural fields, factories, and concentrated feeding operations are created, these healthy ecosystems will take on more nutrients from runoff, causing eutrophic conditions (Bhagowati & Ahamad, 2019). Eutrophication is a process in which water bodies receive excess nutrients (Rast & Thornton, 1996). The increase of nutrients can occur naturally in the environment or it can be accelerated by anthropogenic activities (Bhagowati & Ahamad, 2019). The excess nutrients such as phosphorus in concentrations of 30-100 micrograms/liter and nitrogen in concentrations of 1000-2000 micrograms/liter causes an overgrowth in algae life, known as a bloom (Bhagowati & Ahamad, 2019; Rast & Thornton, 1996)**.** These surface-level blooms grow to such densities that they block sunlight in other primary producers lower down in the water column, thus reducing the production of oxygen through photosynthesis. Eventually, the algal bloom dies off and is consumed by heterotrophic bacteria allowing them to overgrow. Heterotrophic bacteria feed on excessive organic matter build-up and through respiration are the primary driver of anaerobic conditions in the water column. Therefore, through blocking photosynthesis by other phytoplankton and plants and stimulating respiration rates by heterotrophic populations, algal blooms cause extremely anaerobic conditions in water systems (Bhagowati & Ahamad, 2019). There is a vast diversity of cyanobacteria and eukaryotic algae that cause harmful algal blooms (HABs) in different

locations. For example, dinoflagellates cause red tide in Florida, freshwater diatoms cause winter blooms in rivers in Korea, and cyanobacteria dominate the HABs in Lake Erie of the Great Lakes (Ho & Michalak, 2015; Jung et al., 2008; Van Dolah et al., 2009). Here, we will concentrate on the cyanobacteria *Microcystis aeruginosa* that wreak havoc on water systems in the US every year through eutrophication-related blooms (U. S. E. P. A. EPA, 2015).

Cyanobacteria

To begin we will review background information about cyanobacteria to gain understanding of the biological and environmental drivers that impact the growth of *Microcystis.* Cyanobacteria, including *Microcystis*, and other eukaryotic algae biomasses are measured by taking pigment concentrations which helps us understand the dominant phytoplankton group throughout the year. In addition, cyanobacteria and eukaryotic algae are affected by environmental factors such as wind, temperature and pH, and irradiance. These factors have an impact on the times of year that different phytoplankton groups dominate the environment.

Phytoplankton are a diverse group of microbial algae that serve as the base of nearly all aquatic food-webs (Ebert et al., 2001). Phytoplankton bloom when nutrients and light conditions are favorable for growth. Researchers measure primary productivity in these regions using chlorophyll-a (Figure 1), which is synthesized by cyanobacteria and other primary producers during photosynthesis (Campbell et al., 1998). Cyanobacteria also synthesize phycocyanin (Figure 1). While chlorophyll-a is synthesized by numerous

organisms, phycocyanin is only synthesized by cyanobacteria and Rhodophyta (Campbell et al., 1998). Phycocyanin can be a great indicator of how many cyanobacterial cells are present in the environment. Chlorophyll-a and phycocyanin concentrations can be used to measure the estimated biomass of eukaryotic algae and cyanobacteria in the ecosystem. On average, a cyanobacterial cell synthesizes about four times the concentration of phycocyanin compared to that of chlorophyll-a (Peng et al., 2018).

Photosynthetic carbon fixation fuels aquatic ecosystems, but some blooms can become harmful when oxygen-consuming heterotrophic activity causes anaerobic conditions, as previously discussed (Havens, 2008). *Microcystis aeruginosa* is a dominant bloom-forming cyanobacterium that contributes to harmful algal blooms (HABs) (Carmichael, 1994b). These HABs not only result in anaerobic conditions but will also affect clean drinking water in nearby cities due to the release of a toxin, known as microcystin, at high concentrations by *M. aeruginosa* (Carmichael, 1997). Microcystins are a cyclic group of hepatotoxins produced by cyanobacteria with two variable locations on the ring **(Figure 2)** (Schmidt et al., 2014). *Microcystis aeruginosa* produces the most common microcystin, microcystin-LR, which has leucine and arginine at the two variable sites **(Figure 2)** (Schmidt et al., 2014). Microcystin is produced by a group of genes in *M. aeruginosa* known as the microcystin synthesis (*mcy)* genes (Krishnamurthy et al., 1989). Mutation of these genes has previously been used to investigate how genetic differences and community composition impact

distinctions between toxic and non-toxic strains of *M. aeruginosa* (Dittmann et al., 1997; Zuo et al., 2018). There are naturally occurring non-toxic strains of *M. aeruginosa* as well. Microcystin is an intracellular compound and is released into the environment only during cell death throughout a bloom period (Hu & Rzymski, 2019). The microcystin molecule is resistant to harsh conditions; thus, removing it from potable water is challenging and expensive (Hu & Rzymski, 2019). These hepatotoxins can make their way up the trophic levels to affect humans and animals in numerous ways (Schmidt et al., 2014). Chronic exposure to this toxin can cause non-alcoholic fatty liver disease, liver inflammation and hemorrhage, and cancer (U. S. E. P. A. EPA, 2015). The World Health Organization (WHO) recommends the guideline for intake or consumption of microcystin-LR be 1.0 microgram/liter or less (U. S. E. P. A. EPA, 2015).

Although the structure and impacts of microcystin-LR have been studied, their function remains unclear. Previous studies have attempted to determine the reason for microcystin production by *M. aeruginosa* (Ross et al., 2006; Rzymski et al., 2020). However, these studies arrived at different hypotheses, one believed it was an antioxidant (Rzymski et al., 2020) and the other a defense mechanism against predation (Ross et al., 2006). More research is needed to illuminate the use of microcystin. In this thesis, we will not investigate the factors that promote microcystin production. Nevertheless, we hope to contribute to the understanding of its production by exploring mechanisms promoting the growth of the cyanobacteria that produce microcystin.

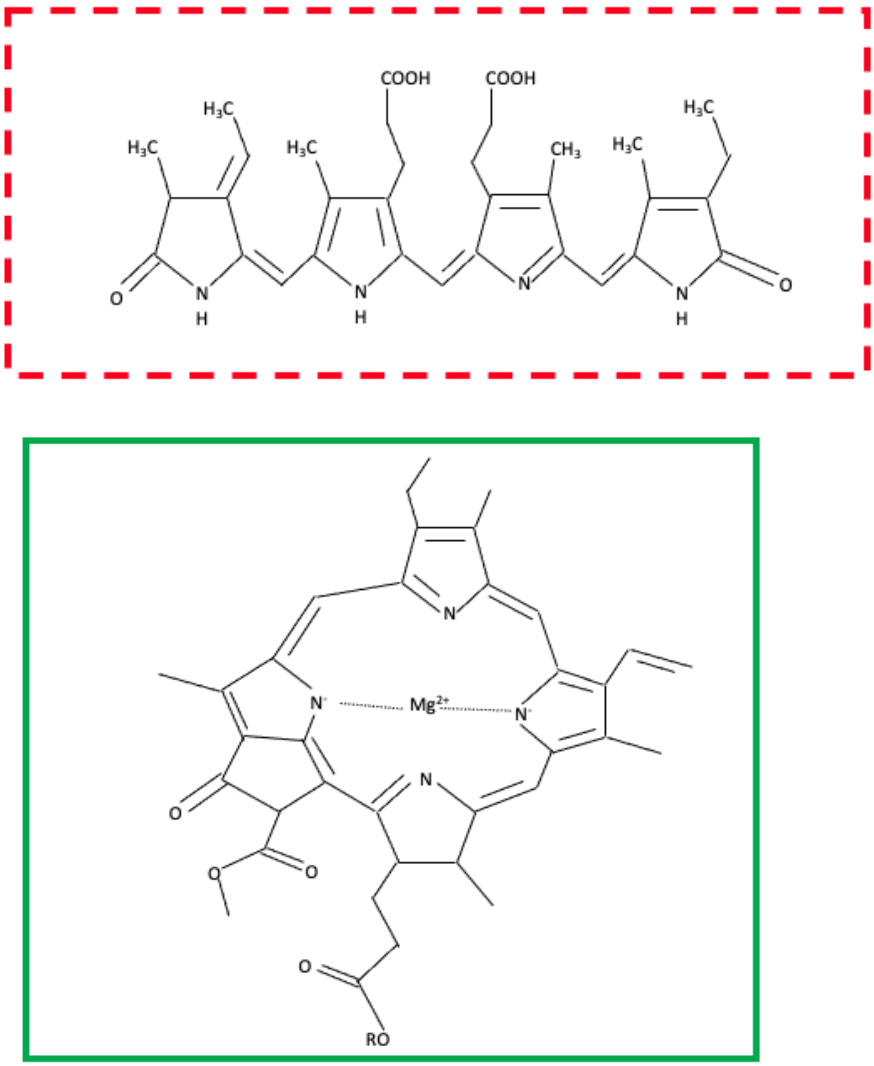

Figure 1: Chlorophyll a versus Phycocyanin
Chlorophyll a is synthesized by all photosynthetic organisms while phycocyanin is synthesized by cyanobacteria. Thus, measurements of the concentrations present in the environment can give insight into the biomass of the organisms present in the community. The chemical structure in the red dashed line box is phycocyanin. The chemical structure in the green solid line box is chlorophyll a. The R group on the chlorophyll a is a long hydrophobic tail (Fernández-Rojas et al., 2014, Björn et al., 2009).

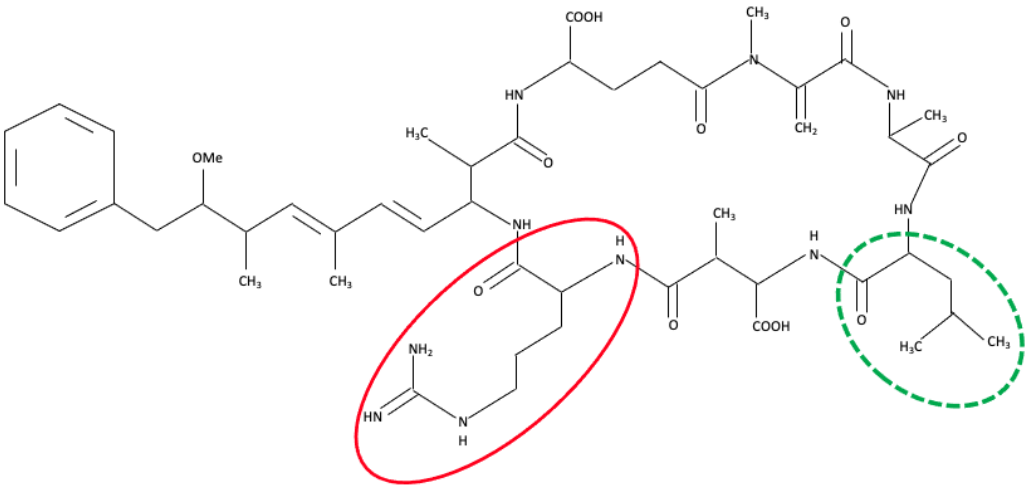

Figure 2: Microcystin
The below figure is of microcystin-LR. In the solid red circle is arginine and in the dashed green circle is leucine. These two amino acids can be switched out with other amino acids making other types of microcystin. These other microcystin types are less toxic to other organisms (Tillett et al., 2000).

Environmental Factors

Wind

Microcystis aeruginosa has a gas vacuole that allows for the cell's movement up and down through the water column (Chunni et al., 2019). This enables the cell to move to locations in the water column that have optimal light and nutrients for maximum growth. However, studies have shown that strong winds can cause mass mixing of the water column especially in shallow lakes (Chunni et al., 2019). Winds speeds as low as 3 meters per second can cause significant near-surface mixing and surface roughness in these shallow lakes (Cao et al., 2006). Thus, affecting the cyanobacterial cell's gas vacuole. *Microcystis aeruginosa* regulate the gas vacuole by modifying the gas vacuolation or by changing the amount of dense components in the cell such as carbohydrates and proteins (Cao et al., 2006). Mixing of the water column causes buoyancy issues with the gas vacuole, which does not allow for *M. aeruginosa* to control where in the water column they are located. Strong winds have been shown to cause enough mixing to break up the cyanobacterial colonies and weaken the cells' ability to grow (Chunni et al., 2019). Therefore, a lack of winds in the environment during certain parts of the year may partially contribute to the intensity and frequency of these harmful algal blooms.

Temperature and pH

The temperature and pH of the environment can affect how species grow and compete in the community. In the environment, cyanobacterial blooms

dominated by *M. aeruginosa* occur in the late summer when the water temperatures are typically at their highest levels (Imai et al., 2009; Paerl & Huisman, 2008; Paerl & Paul, 2012). Studies have shown that *M. aeruginosa* prefers to grow and compete at high temperatures and high pH (Yang et al., 2018). In these studies, *M. aeruginosa* was at a competitive advantage in temperatures between 20 to 30 degrees Celsius and in neutral and weakly alkaline conditions (pH 7-9) (Yang et al., 2018). *Microcystis aeruginosa* lowers its growth rate starting at 35 degrees Celsius. These studies have also found that inside these massive colonies formed by *M.* aeruginosa the pH is around 10 (Fang et al., 2018). At this pH, oxygen bubbles form and will provide extra buoyancy for these large colonies. Under the colonies, anaerobic conditions form killing off other organisms that rely on the oxygen in the water column for survival (Fang et al., 2018). Taking these factors into consideration, cyanobacterial blooms may grow in frequency and intensity as the globe continues on its current warming trend and the pH continues to change.

Irradiance

Irradiance changes throughout the year with the different seasons. For example, in the Northern Hemisphere, during the winter months, the irradiance is low, but in the summer months, the irradiance is high. *Microcystis aeruginosa* bloom during the summer months and have higher growth rates with experimentally controlled irradiance (Fang et al., 2018). *Microcystis aeruginosa* even have a gas vacuole that allows them to move through the water column to

locations of optimal light for maximal growth (Chunni et al., 2019). Studies have shown that under high light conditions, *M. aeruginosa* increase their gas vacuole size and carbohydrate concentration in the cell (Brookes & Ganf, 2001). At high irradiance, *M. aeruginosa* can create these colonies that were mentioned above and block the sunlight from penetrating into the water column. This blocking of sunlight prevents other primary producers from their required irradiance needed for photosynthesis to occur and these other primary producers die off. However, in low light conditions, *M. aeruginosa* does not have a competitive advantage and tend to die off when in unicellular form rather than colony form (Wu & Song, 2008; M. Zhang et al., 2011). Thus, irradiance can be a limiting resource for these cyanobacterial blooms. Irradiance also affects other properties that affect these cyanobacterial cells, such as elevating the temperature and pH and allowing for higher reactive oxygen species concentrations (Fang et al., 2018; Zheng et al., 2019).

Competition: Eukaryotic Algae

Competitors to *M. aeruginosa* include other eukaryotic algae such as diatoms in freshwater ecosystems. Diatoms are unicellular photosynthetic algae present in freshwater and saltwater ecosystems (Medarevic et al., 2015). The cells are of a variety of different shapes and sizes (Kale & Karthick, 2015). These algae produce silica cell walls known as frustule (Kale & Karthick, 2015). Researchers believe that these frustules help defend against predation and protect the organism against light (Aguirre et al., 2018; Spillane, 2016). During

photosynthesis, these eukaryotic algae produce chlorophyll a and chlorophyll c along with multiple xanthophylls, which can all be measured to estimate the biomass of eukaryotic algae in the community (Kale & Karthick, 2015). Although diatoms are present for most of the year, diatoms tend to bloom in freshwater ecosystems in the late spring and throughout summer. During this time, diatoms are the dominating primary producer (Reynolds, 1973). Diatoms are also very efficient at acquiring nutrients, while other organisms such as *Microcystis* are better at defending against predation (Lürling, 2021). Understanding how these eukaryotic algae compete with cyanobacteria for resources can be very insightful into how cyanobacterial cells reach such high biomasses allowing them to dominate the community.

Predation: Zooplankton

Zooplankton are a herbivorous species. Zooplankton have been used to study cyanobacterial blooms because of their presence in lake environments and their consumption of phytoplankton (Urrutia-Cordero et al., 2016). These zooplankton can be used to investigate their top-down pressure on the phytoplankton groups, including *M. aeruginosa.* However, zooplankton's effectiveness in controlling cyanobacterial blooms has been controversial (Kemal A. Ger et al., 2014; Hansson et al., 1998; Urrutia-Cordero et al., 2016). Although cyanobacteria, including *M. aeruginosa*, have been known to limit zooplankton communities' fitness due to their toxin release and low nutritional value (Urrutia-Cordero et al., 2016; Wilson et al., 2006).

Microcystis aeruginosa also forms colonies that make grazing difficult due to the size of the colony in comparison to the size of the zooplankton (Lampert, 1987; Schmidt et al., 2014; Urrutia-Cordero et al., 2016). Colony formation can occur in response to biotic factors such as grazers, heterotrophic bacteria, and polysaccharide production (Xiao et al., 2018). However, the effects of grazing on colony formation vary depending on the type of zooplankton present. Some grazers have infochemicals that are released into the environment, which are hypothesized to cause colony formation (Xiao et al., 2018). Microcystin-LR has been hypothesized to cause colony formation, and *M. aeruginosa* is known to release this microcystin in the presence of some zooplankton species (Lürling et al., 2013; Xiao et al., 2018). Previous studies aim to determine if the mechanical act of grazing on *M. aeruginosa* releases enough microcystin, via sloppy feeding, into the environment for colony formation to protect against further predation (Xiao et al., 2018). We plan to investigate the role that *M. aeruginosa's* inherent ability to resist zooplankton predation may cause their domination over other phytoplankton groups during late summer months in lake ecosystems.

Modeling of Lake Ecosystems

Experiments can be completed using three approaches: laboratory, field work, and modeling. Laboratory experiments are great for having a high degree of control over factors and easy manipulation of specific variables in the experiment. However, laboratory experiments lack the real-world environmental settings and variability seen in the field experiments. Unfortunately, field

experiments are hard to manipulate variables due to the scale of the system. We believe that modeling can be used to supplement the limitations in both laboratory and field experiments. Modeling can easily manipulate variables on large scales and can use parameters and data from the laboratory and field experiments to help guide the model development.

In building our model we needed to investigate the three main types of models in the literature and determine which of those model types best fits our question. The three types of models are prediction models (individual-based and machine-learning), biogeochemical models, and theoretical models. Individual-based models (IBMs) use population-average cell quotas and apply them to individual algal cells to produce population-level results (Hellweger & Kianirad, 2007). However, these individual based models do not take into account competition for nutrients between different phytoplankton or cyanobacteria groups. Machine-learning prediction models like those by The Prediction Lab (thepredictionlab.com) use data and a Bayesian modeling approach to make 7-day predictions for HABs. Biogeochemical models and hydrodynamic models have been coupled to account for hydrodynamics and ecological processes. Of major interest, is the Framework for Aquatic Biogeochemical Model (FABM) which allows for biogeochemical models to be built as stand-alone models and can be linked to ecosystem models such as ERSEM (marine model) and PCLake (freshwater) (Bruggeman & Bolding, 2014). Finally, theoretical models can be used to make ecological predictions about competition for resources, predation,

and other interactions occurring in communities (Armstrong & McGehee, 1980; Holt et al., 1994; Hutchinson, 1961; Tilman, 1982). These models all have their positive and negative contributions to our project. However, none of these models individually give the general framework to incorporate all the different drivers (light, nutrient enrichment, and predation) we want to investigate.

We have found several models from the last 10-15 years that have accounted for physical dynamics and some ecological aspects. For example, Jiang et al. 2015 used a physical model known as Finite Volume Coastal Ocean Model (FVCOM), which is a sub-model of FABM, to investigate the impact of river inputs and wind dynamics on nutrient advection and vertical mixing (Jiang et al., 2015). This study used nutrients to understand how variation in nutrient loading and mussel density could impact zooplankton predation of phytoplankton (Jiang et al., 2015). Another study, by Zhang et al. 2008, used a hydrodynamic and water quality model to investigate the impacts of different mussels on the phytoplankton populations in Lake Erie (H. Zhang et al., 2008). Through our research, we have not found a biogeochemical model to make predictions for a diamond food-web model that allows for variation of environmental conditions in lake ecosystems.

Food-web Modeling

Of specific interest for our project is a food-web model, which is a type of theoretical model. Food-webs are a quantitative way to think about the environmental dynamics and pressures in an ecosystem (Lindeman, 1991).

Understanding the food-web of an ecosystem can give valuable insight into how food-web dynamics will change when external environmental variables shift. Bottom-up influences, such as nutrient control or enrichment, and top-down influences, such as higher trophic level organisms feeding upon the lower trophic levels, are ways to investigate the complexities of blooming populations and how to selectively control those blooming populations (Tambling et al., 2015).

The ecological interactions driving selection of cyanobacteria are poorly understood. We know that nutrient enrichment drives the selection of cyanobacteria. A major focus of theoretical and applied work in this area has been on nutrient limitation. These studies have invoked theories dating back to the 1940s to describe populations being controlled by nutrient limitation (Lindeman, 1991). Yet, predator-prey interactions and relationships are seen everywhere in nature including in microbial communities. Predator-prey interactions may play a major role in selecting harmful cyanobacteria in productive lakes, but relatively little theoretical work has been applied specifically to this problem. Food-web models suggest changes in how population densities of predators and prey drive shifts in selective pressure (Tambling et al., 2015). Higher nutrient input may drive enhanced pressure for defensive groups when high cell densities lead to high contact rates between predators and prey. Differential selection along nutrient supply gradients is expected when there is a trade-off between resource acquisition and defense against predation (Tilman, 2004). These ideas are well-known in the theoretical literature; however, they

have not been invoked in a modeling framework of lake ecosystems to explain why cyanobacteria are selected at high population densities. We will consider this selection in context of variable environmental forcing such as variable temperature.

Questions and Hypothesis

Question: What environmental conditions cause *Microcystis aeruginosa* to outcompete eukaryotic algae?

We hypothesize that enriched resource inflow and temperature selects for defense against predation, which may be a major reason why Microcystis aeruginosa are selected for in hyper-eutrophic lakes.

CHAPTER TWO: ENVIRONMENTAL DATA ANALYSIS

Lake Erie and Environmental Data

To guide our model development appropriately we need to understand the environmental data. We used data from Lake Taihu in China during 2005 to guide our question about seasonal succession in the phytoplankton-cyanobacteria communities (Ke et al., 2008). As seen in the data from Lake Taihu (**Figure 3**), there is a seasonal succession between eukaryotic algae and *Microcystis* (Ke et al., 2008). The eukaryotic algae have a higher biomass throughout the year until late May when there is a transition from eukaryotic algae to *Microcystis* dominating the community.

In looking at data from Lake Erie, a priority is to determine how general this successional pattern is. Therefore, we used data from NOAA and the EPA's CDX data exchange for time series data from Lake Erie (**Figure 4**) (Burtner et al., 2019; U. S. EPA, 2019). The NOAA time series data was from buoys in the western basin in Lake Erie and was taken from 2012 through 2018. This time series data collected total phosphorus concentrations, pigment concentrations (chlorophyll-a and phycocyanin), ammonia, nitrate, and nitrite concentrations as well as microcystin concentrations and other environmental conditions. Time series data from the EPA's CDX data exchange program was collected in all three basins of Lake Erie and was collected from 1997 to 2018. This time series data collected number of individual counts and biomass

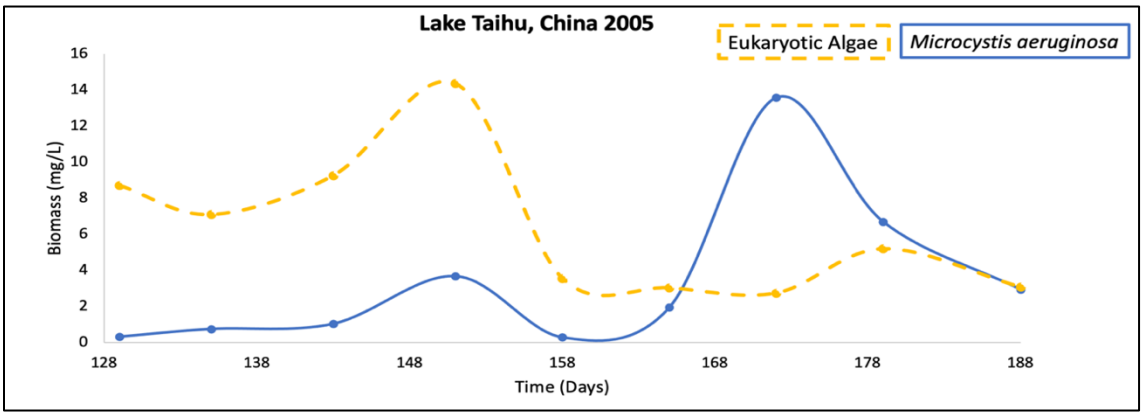

Figure 3: Lake Taihu Data
Data from Lake Taihu showing successional pattern between eukaryotic algae and *Microcystis* (Ke et al., 2008).

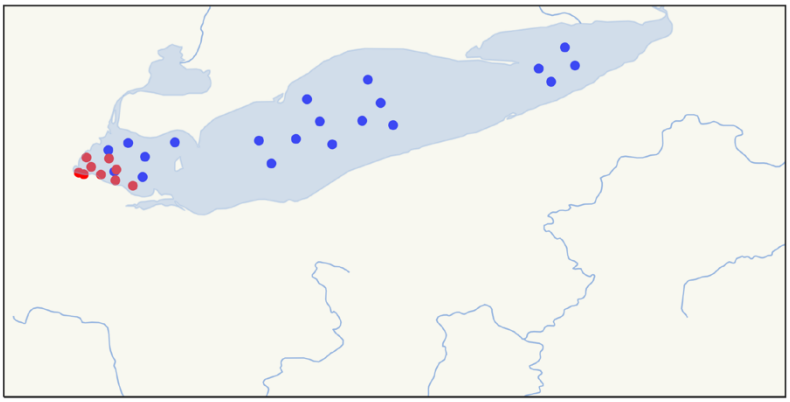

Figure 4: Lake Erie Sampling Locations
Sampling locations (latitude, longitude) in Lake Erie. Red markers measured nutrient and pigment concentrations. Blue markers measured biomass of zooplankton (Burtner et al., 2019; U. S. EPA, 2019).

measurements for several different zooplankton species. For simplicity, in this analysis we combined all the zooplankton species biomasses to get an overall understanding of the changing zooplankton biomass throughout the year. Our analysis uses the pandas library in Python to organize and analyze our data.

In order to gain a full understanding of the different patterns in the nutrient and pigment concentrations we analyzed the data per year and throughout each year **(Figure 5).** Some yearly patterns seem to emerge, but it is difficult to tease through the importance of those potential patterns when looking at the data as a whole. We also wanted to get an understanding of both bottom-up and top-down data in the environment. Thus, our analysis led us to investigating how the predators' biomass in Lake Erie changes throughout the year **(Figure 6)**. Using data from the EPA, we had biomass data for multiple species of zooplankton (U. S. EPA, 2019). Interannually, there is no major change in the biomass of the zooplankton present in Lake Erie **(Figure 6).** However, total zooplankton biomass is higher in August of each year.

To inform our model about the changes in water clarity throughout the year we wanted to understand the changes in secchi depth over each year of the study. As seen in **Figure 7**, it is difficult to decipher if there is an interannual or intra-annual change or pattern in water clarity (Burtner et al., 2019).

Overall, as seen in the figures above, it is difficult to determine if there are any patterns present in the data when looking at the data as a whole. In order to

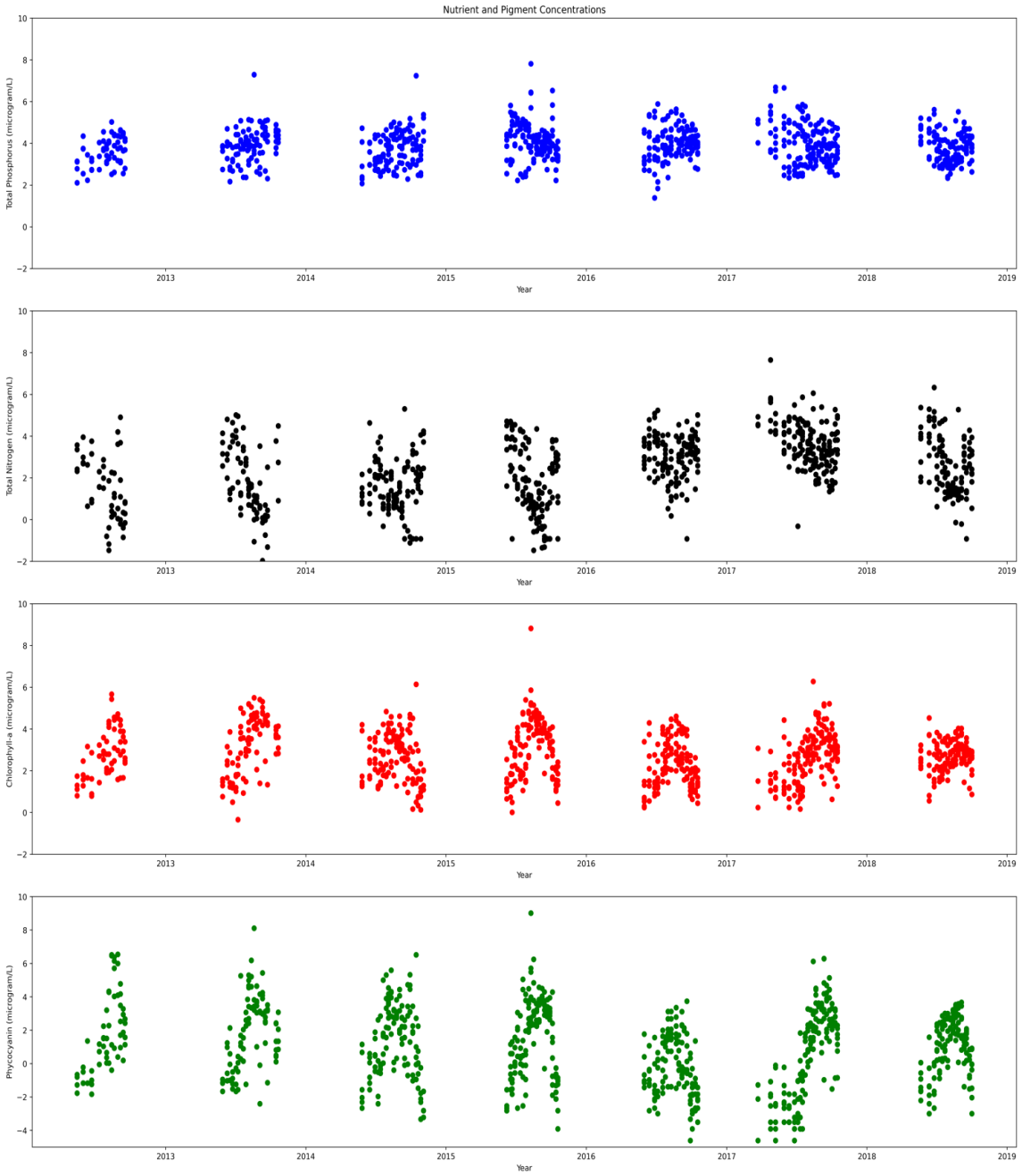

Figure 5: Lake Erie Nutrient and Pigment Concentrations
A scatter plot of the total phosphorus (blue), total nitrogen (black), chlorophyll-a (red), and phycocyanin (green) concentrations for each month throughout each year (Burtner et al., 2019).

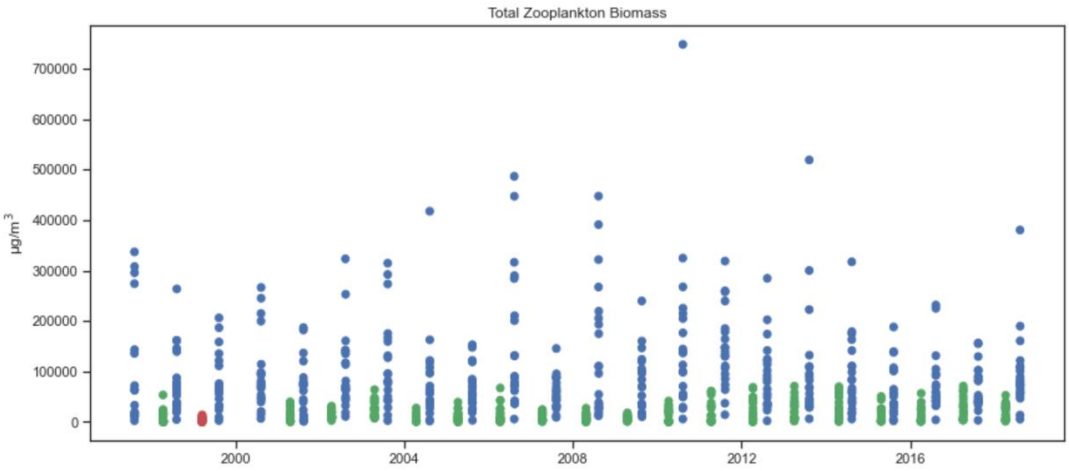

Figure 6: Lake Erie Zooplankton Data
A scatter plot of the total zooplankton biomass comparing March (red), April (green), and August (blue) (U. S. EPA, 2019).

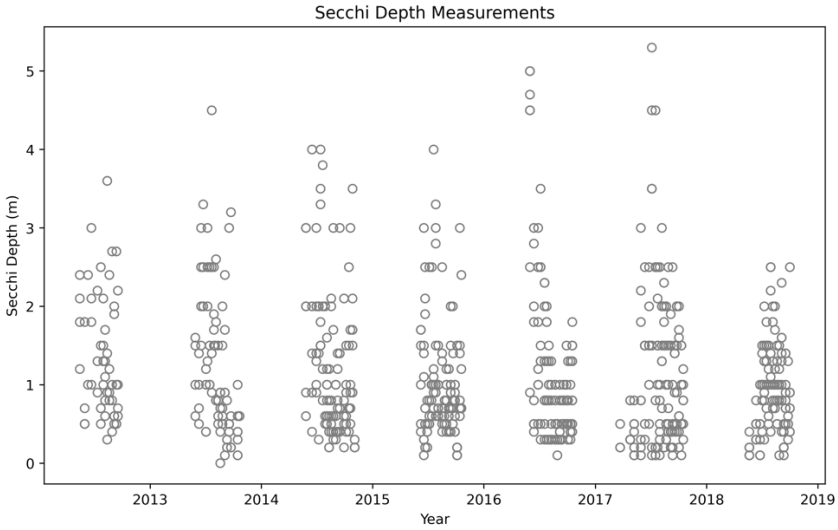

Figure 7: Secchi Depths
A scatter plot of the secchi depths measured each year (Burtner et al., 2019).

determine and analyze any patterns we need to break our data down for inter-annual analysis to determine if there are significant changes from one year to another. We also need to analyze this data intra-annually to determine if there are significant patterns occurring throughout the year.

Inter-annual Data Analysis

Our first analysis of the data was done inter-annually to determine if there are patterns present from one year to another. Changes in water clarity can be helpful in indicating the concentrations of nutrients, biomass of phytoplankton, and the amount of sunlight reaching lower depths in the water column. We use changes in secchi depth to indicate when changes in the water column were occurring. Inter-annually **(Figure 8)** there seems to not be much of a change from one year to another in water clarity. We compared the ratio of phycocyanin to chlorophyll-a in relation to the biomasses of cyanobacteria and eukaryotic algae present in the environment. Interannually, there is a consistent ratio telling us that there is no massive change in either chlorophyll-a or phycocyanin from one year to the next **(Figure 9).**

Interannually, there seems to be no major changes or patterns that occur for the nutrients **(Figure 10 and Figure 11).** This result tells us that there is no major depletion of phosphorus or nitrogen in the environment during monitoring and that the cyanobacterial blooms are staying relatively stable in biomass.

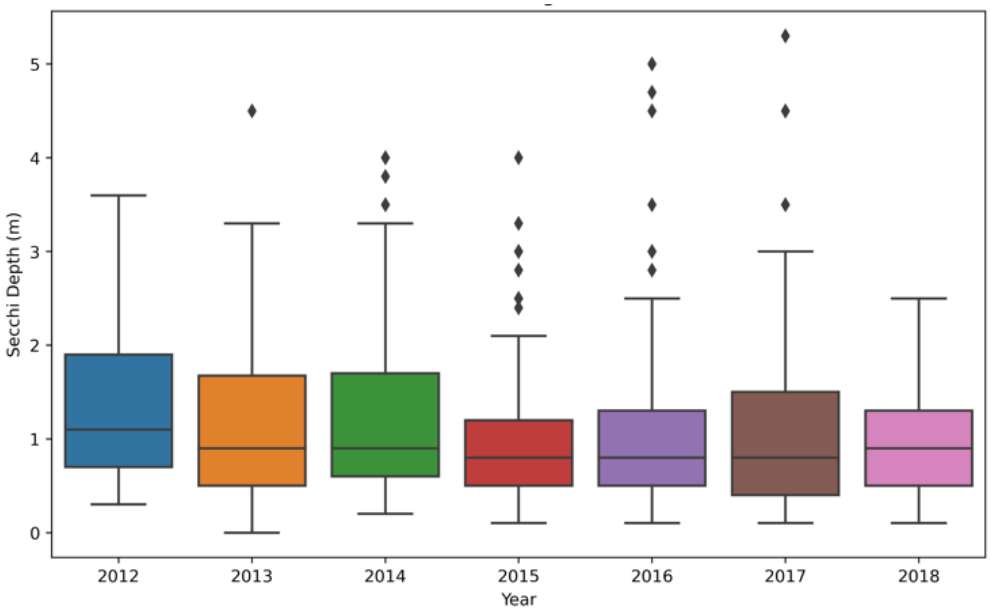

Figure 8: Interannual Secchi Depth
A box plot of the secchi depths each year (Burtner et al., 2019).

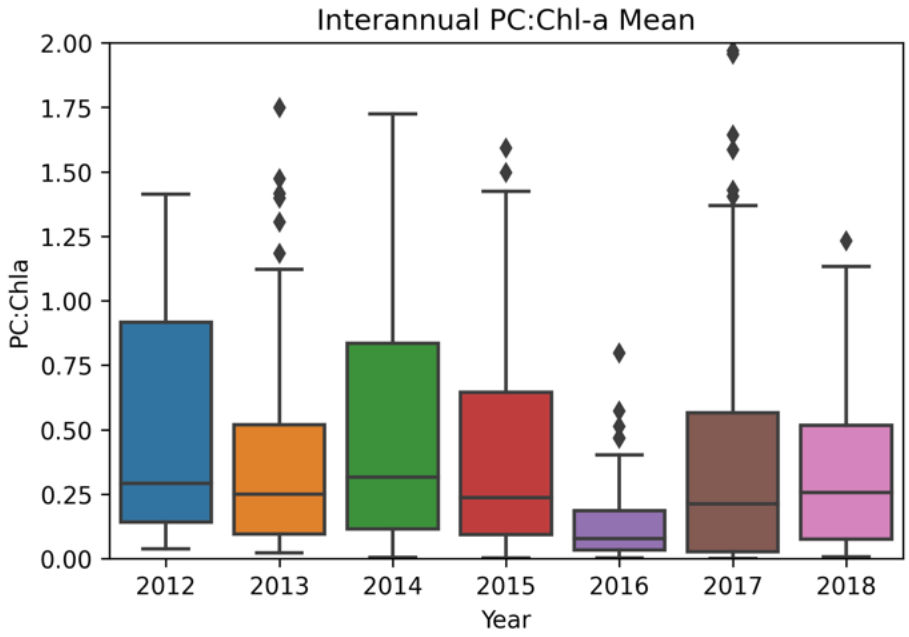

Figure 9: Interannual Phycocyanin to Chlorophyll-a Ratio
A box plot of the phycocyanin to chlorophyll-a ratio each year (Burtner et al., 2019).

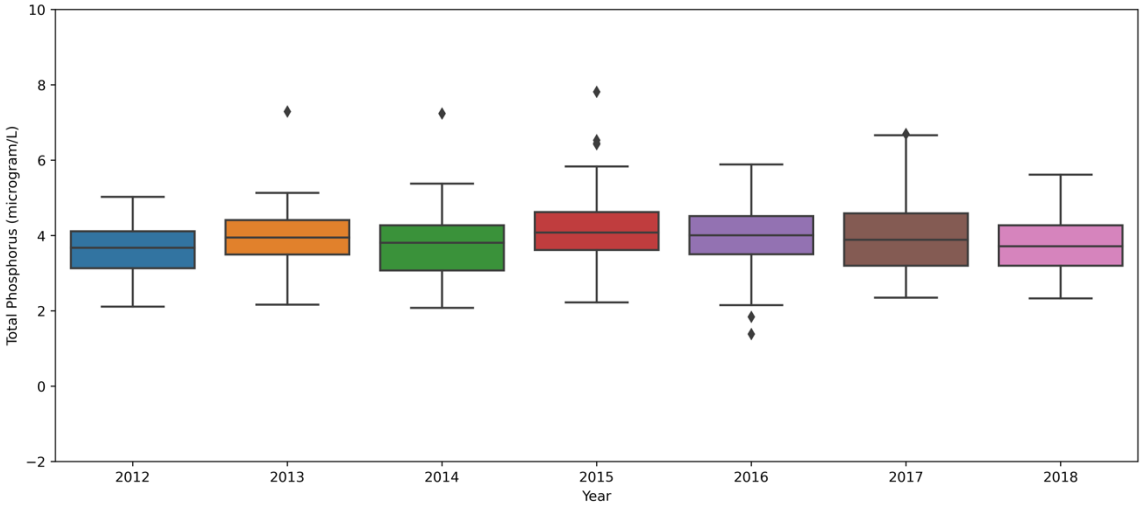

Figure 10: Interannual Phosphorus Concentration
A box plot of the phosphorus concentration each month through the years (Burtner et al., 2019).

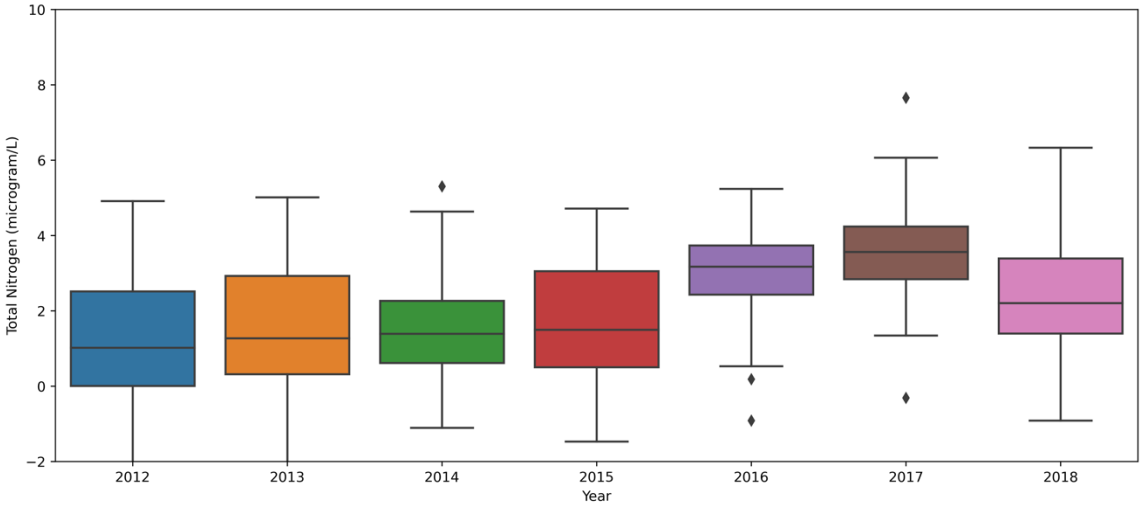

Figure 11: Interannual Nitrogen Concentration
A box plot of the nitrogen concentration each month through the years (Burtner et al., 2019).

Intra-annual Variability

One major goal given the intra-annual pattern for the data was to determine how the phytoplankton and cyanobacteria biomasses change throughout the year. Since we don't have these specific measurements of biomasses, we used the concentrations of the pigments that these groups synthesize. The time series sampling was taken each year from March through November. In our analysis, regardless of the year that the data was taken, we grouped it by the month and then calculated the median, 75^{th} percentile, and 25^{th} percentile per month for the chlorophyll-a concentration and the phycocyanin concentrations. This helped us visualize how the concentrations of each pigment changes throughout the year **(Figure 12).** In **Figure 12**, we see that there is a peak of pigment concentration for both pigments in August-September. This fits with observations that *Microcystis* blooms typically occur in the environment during those late summer months.

Since cyanobacteria synthesize both chlorophyll-a and phycocyanin, one of our main questions about this data was how much of the chlorophyll-a is synthesized by cyanobacteria. Using the Peng *et al.* study we estimated that each cyanobacterium cell synthesizes on average four times more phycocyanin than chlorophyll-a (Peng et al., 2018). Thus, with this estimation we wanted to compare the concentrations of phycocyanin with the concentrations of chlorophyll-a; where the chlorophyll-a concentration excludes that synthesized by cyanobacteria **(Figure 13)**. **Figure 13**, left panel, shows the comparison between

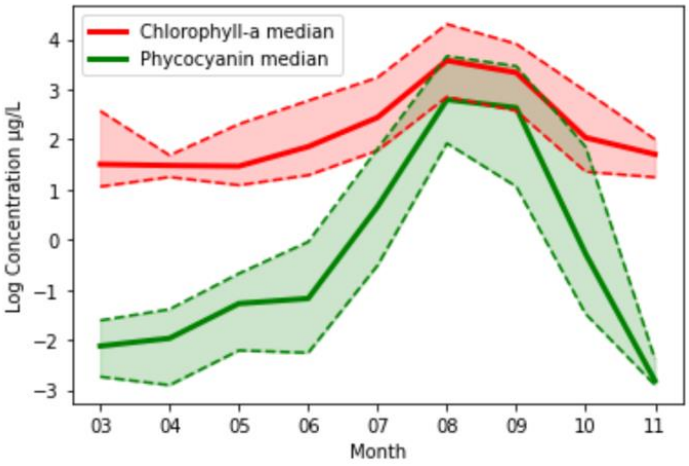

Figure 12: Intra-annual Pigment Data
The data was grouped by month (regardless of the year that it was taken) and the median of each month was graphed (Burtner et al., 2019). The red solid line represents the median chlorophyll-a concentration. The upper and lower dashed lines represent the 75th and 25th percentiles, respectively. The green solid line represents the median phycocyanin concentration. The upper and lower dashed lines represent the 75th and 25th percentiles, respectively.

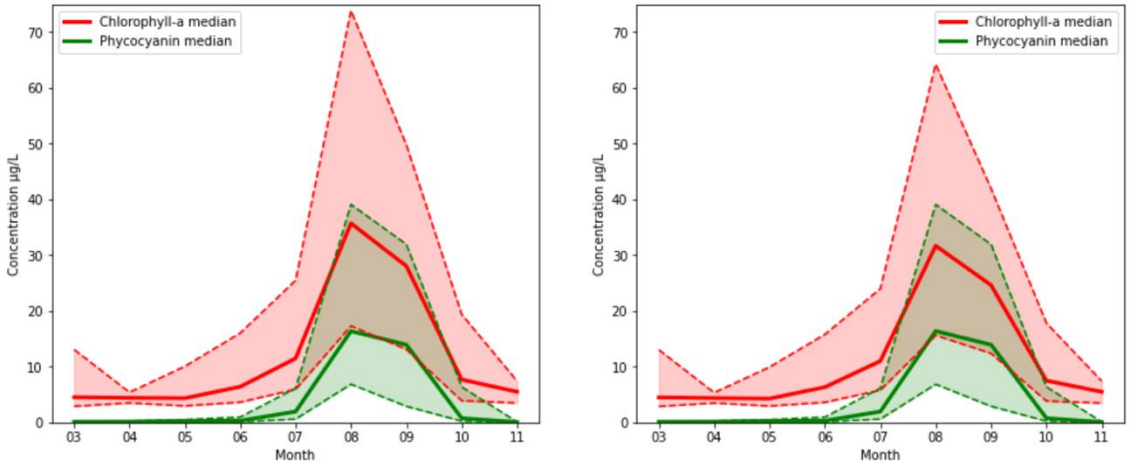

Figure 13: Intra-annual Median Pigment Concentration Comparison
Comparison of the median chlorophyll-a concentrations and the median phycocyanin concentrations throughout the year (Burtner et al., 2019). The red solid line represents the median chlorophyll-a concentration. The upper and lower dashed lines represent the 75th and 25th percentiles, respectively. The green solid line represents the median phycocyanin concentration. The upper and lower dashed lines represent the 75th and 25th percentiles, respectively.

the full concentration of chlorophyll-a (red) and phycocyanin (green); while the right panel shows the comparison of chlorophyll-a (red), without chlorophyll-a synthesized by cyanobacteria, and phycocyanin (green). Overall, this shows us that during the cyanobacteria bloom in August-September other chlorophyll-a producing organisms are still present in the environment.

Next, we wanted to understand the limiting resource in the ecosystem. For this analysis, we compared the total phosphorus concentrations with the nitrogen concentration. In the data, we were given the total phosphorus (including total dissolved phosphorus and soluble reactive phosphorus), nitrate + nitrite, and ammonia. In order to compare these nutrients, we combined the nitrate + nitrite and ammonia concentrations. **Figure 14** shows our comparison of median phosphorus (black) and nitrogen (blue) concentrations. We were surprised to see the major draw down of the nitrogen while the phosphorus concentration stays relatively constant throughout the year.

In order to understand the comparison between the median nitrogen and phosphorus concentrations, we calculate the nitrogen to phosphorus molar ratio. This calculation was done for each data point, and then we calculated the average nitrogen to phosphorus molar ratio per month **(Table 2.1 and Figure 15)**. **Table 2.1** shows that there is either a major draw down of nitrogen or a major influx of phosphorus from July to August which corresponds to the largest growth in phycocyanin concentration during the study. In comparison to Redfield's ratio **(Figure 15),** we approximate that the community is limited by

phosphorus until August and then it is nitrogen limited when the nitrogen to phosphorus ratio drops below Redfield's ratio. However, this does not seem to be a typical pattern in the data. Some studies show that laboratory experiments of *Microcystis* growth in high N:P (~40) conditions drive the inorganic N:P ratio even higher (~400) which is not consistent with the pattern seen in the data from Lake Erie (Zhu et al., 2015). Intra-annually, zooplankton biomass increases throughout the year **(Figure 16).** This increase occurs from March to August. The increase in biomass correlates each year during the drawdown of nutrients and the increase in phytoplankton biomass.

Our data analysis shows that during summer there is a slight draw down of nutrients during an increase in the biomass of both eukaryotic algae and *Microcystis.* As the biomass of phytoplankton increases, we find an increase in the biomass of zooplankton. As the zooplankton biomass increases, we see an increase in the phycocyanin to chlorophyll-a ratio **(Figure 17).** Thus, supporting the growth of cyanobacteria. Laboratory data shows that *Microcystis* are poorly grazed on by zooplankton (Ger et al., 2019; Lürling, 2021). These laboratory data and our environmental data analysis led to the hypothesis that shifts in resource inflow select for defense against predation, which may be a major reason why *Microcystis aeruginosa* are selected for in hyper-eutrophic lakes.

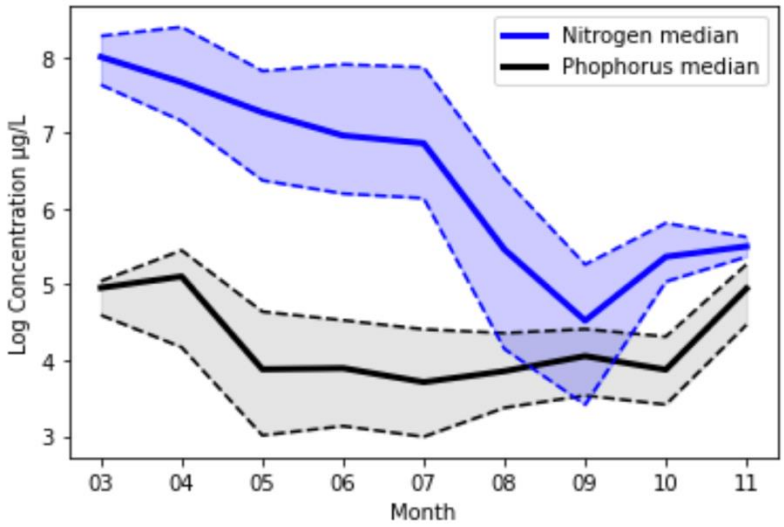

Figure 14: Intra-annual Nutrient Concentrations
Comparison of the median phosphorus and nitrogen concentrations throughout the year. The blue solid line represents the median nitrogen concentration (Burtner et al., 2019). The upper and lower dashed lines represent the 75th and 25th percentiles, respectively. The black solid line represents the median phosphorus concentration. The upper and lower dashed lines represent the 75th and 25th percentiles, respectively.

Table 2.1: Concentrations Ratio Table

Month	Molar N:P Ratio	Mass N:P Ratio	PC: Chl a Ratio
03	36.701017	24.207054	0.015807
04	31.098565	20.511820	0.030392
05	46.991787	30.994583	0.081912
06	46.642990	30.764526	0.083291
07	44.618819	29.429434	0.290339
08	15.023705	9.909252	0.853273
09	5.214089	3.439080	0.568227
10	10.206752	6.732113	0.247493
11	3.381040	2.230047	0.016938

Calculation of the nitrogen to phosphorus concentration and change in the phycocyanin to chlorophyll-a concentrations monthly (Burtner et al., 2019).

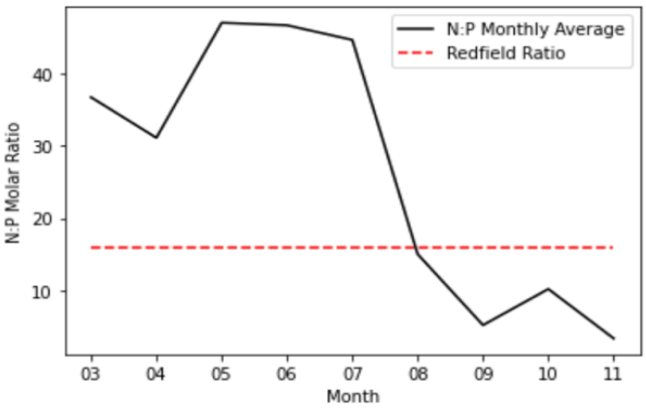

Figure 15: Intra-annual Nitrogen to Phosphorus Ratio
The monthly average molar nitrogen to phosphorus ratio (black solid line) in comparison the Redfield's ratio (red dashed line) of 16:1 (Burtner et al., 2019).

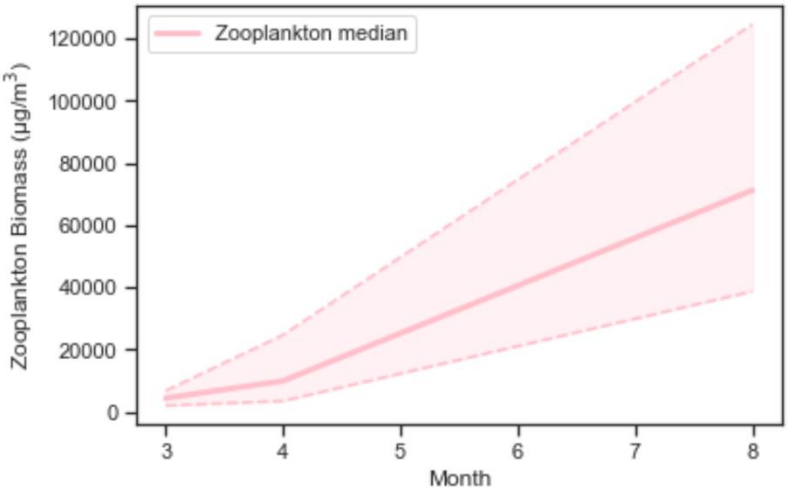

Figure 16: Intra-annual Zooplankton Biomass
Intra-annual median zooplankton biomass throughout the year. The pink solid line represents the median zooplankton biomass concentration (U. S. EPA, 2019)). The upper and lower dashed lines represent the 75th and 25th percentiles, respectively.

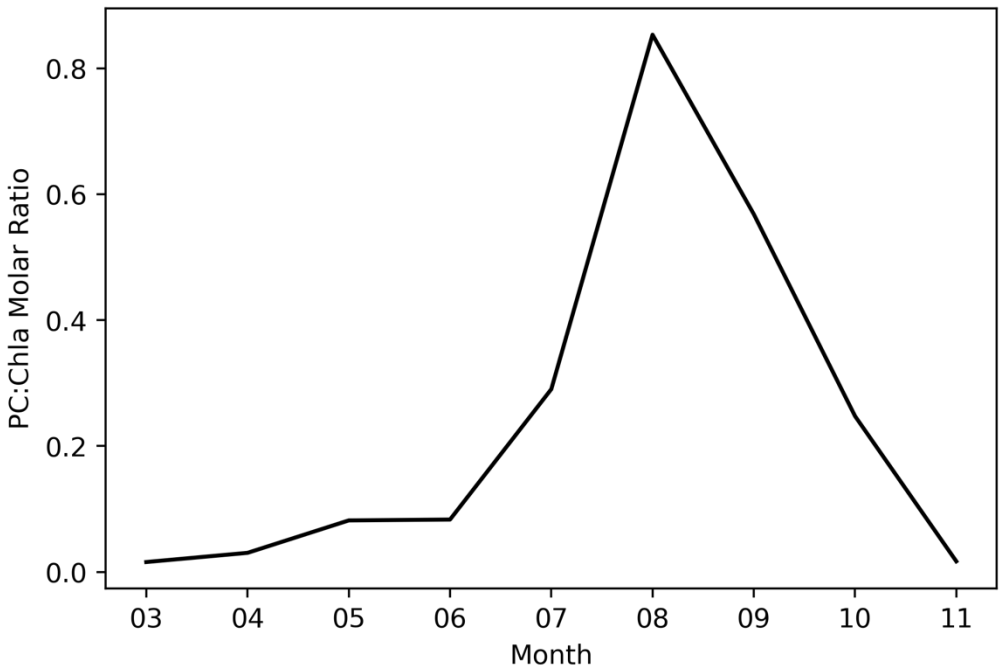

Figure 17: Intra-annual Phycocyanin to Chlorophyll-a Ratio
The monthly average phycocyanin to chlorophyll-a ratio (Burtner et al., 2019).

CHAPTER THREE: THEORETICAL FOOD-WEB MODELING, NUTRIENT CONCENTRATION, AND TEMPERATURE STUDY

The Model

Using the information from our analysis of time series data in Lake Erie, we configured a model that we believe responds to our research question and can be used to investigate our main hypothesis, that resource enrichments drive a higher contact rate between predators and prey, shifting selection pressure toward species groups better at defending against predation, leading to selection of *Microcystis* in lake ecosystems. This model, as seen in **Figure 18**, includes a supply rate of nitrogen (S_R), a pool of nitrogen (N), two producer groups (P_1 and P_2) that pull from that nitrogen pool, and a consumer group (C) that is a predator for both producer groups. Our community structure can be modeled using the equations in the **Equations 1-4**. These first order differential equations comprise a non-linear system. Each equation is the change in a state variable (Nitrogen, Producer 1, Producer 2, and Consumer) over time. The parameters used in each equation and their units can be found in **Table 3.1**.

Individually, the equation for change in Nitrogen over time has an external input of the supply rate (S_R, **Table 3.1**) and outputs from the nitrogen uptake from each producer group (μ_1 and μ_2, **Table 3.1**) and a nitrogen degradation (δ_N, **Table 3.1)**. The producer groups have an input from the uptake of nutrients by the group (μ_1 and μ_2, **Table 3.1**) and outputs from the predation by consumers (φ_1 and φ_2, **Table 3.1**) and a background loss rate (δ_1 and δ_2, **Table 3.1)** from other events not included in this model. Finally, the consumer group has inputs

from consuming the producer groups ($\varepsilon_1\varphi_1$ and $\varepsilon_2\varphi_2$, **Table 3.1**) and an output of background loss rate (δ_C, **Table 3.1)** from other events not included in this model.

$$\frac{dN}{dt} = \underbrace{S_R}_{\text{Supply rate}} - \underbrace{\mu_1 N P_1 - \mu_2 N P_2}_{\text{Uptake by Producers}} - \underbrace{\delta_N N}_{\text{Nitrogen removal}} \quad (1)$$

$$\frac{dP_1}{dt} = \underbrace{\mu_1 N P_1}_{\text{Uptake of resource}} - \underbrace{\varphi_1 P_1 C}_{\text{Predation}} - \underbrace{\delta_1 P_1}_{\text{Background loss}} \quad (2)$$

$$\frac{dP_2}{dt} = \underbrace{\mu_2 N P_2}_{\text{Uptake of resource}} - \underbrace{\varphi_2 P_2 C}_{\text{Predation}} - \underbrace{\delta_2 P_2}_{\text{Background loss}} \quad (3)$$

$$\frac{dC}{dt} = \underbrace{\varepsilon_1 \varphi_1 P_1 C + \varepsilon_2 \varphi_2 P_2 C}_{\text{Consumption of Producers}} - \underbrace{\delta_C C}_{\text{Background loss}} \quad (4)$$

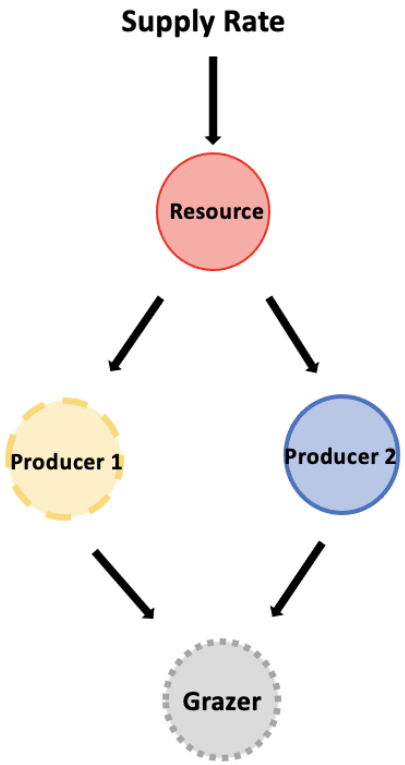

Figure 18: Community Structure Diagrams
These diagrams are basic community structure graphics used in ecology to visually depict what interactions are occurring in the system. In this figure, supply rate is the nutrient supply into the system (i.e., nitrogen, phosphorus, etc.), the resource pool is nutrient concentrations present in the environment, producer 1 and producer 2 are primary producers such as eukaryotic algae and cyanobacteria. Finally, the grazer is the zooplankton, and, in this case, the grazing group feeds on both pools of producers.

Table 3.1: Table of Symbols

Symbol	Symbol meaning	Units
S_R	Supply rate	$\frac{mmol\ N}{day\ m^3}$
μ_1, μ_2	Resource affinity	$\frac{m^3}{day\ mmol\ N}$
φ_1, φ_2	Interaction strength	$\frac{m^3}{day\ mmol\ N}$
$\delta_N, \delta_1, \delta_2, \delta_C$	Background death rate/ resource degradation	$\frac{1}{day}$
$\varepsilon_1, \varepsilon_2$	Transfer efficiency	$\frac{mmol\ N}{mmol\ \ N}$
$\frac{dN}{dt}$	Change in nitrogen over time	$\frac{mmol\ N}{day\ m^3}$
$\frac{dP_1}{dt}, \frac{dP_2}{dt}$	Change in producer 1 and producer 2 over time	$\frac{mmol\ N}{day\ m^3}$
$\frac{dC}{dt}$	Change in consumer over time	$\frac{mmol\ N}{day\ m^3}$

Parameters and state variables used in the mathematical model including the symbol, the meaning of the symbol, and the mathematical units of the symbol.

Methods

In our experimental approach, we will simulate resource enrichment **(Figure 19)** to investigate the sensitivity of community structure using contrasting food-web structures; one without a consumer and one with a consumer (Model 1A and Model 1b, respectively). Producers, P_1 and P_2, have contrasting traits with P_1 strong in resource acquisition and P_2 strong in defense against predation (Model 1B). In these models, P_1 and P_2 are analogs of eukaryotic algae and *M. aeruginosa,* respectively. All parameter values used in our model simulations can be found in **Table 3.2**. The goal of our experiment is to determine whether nutrient enrichment can drive a switch from P_1 to P_2 with and without top-down control.

Results and Discussions

We begin with a mathematical model in which two producers compete for a resource, which is supplied at a piecewise constant rate. The system can be characterized using the scheme in **Figure 20** and **Equations 5-7**:

$$\frac{dR}{dt} = \underbrace{S_R}_{\text{Supply rate}} - \underbrace{\mu_1 R P_1 - \mu_2 R P_2}_{\text{Uptake by Producers}} \quad (5)$$

$$\frac{dP_1}{dt} = \underbrace{\mu_1 R P_1}_{\text{Uptake of resource}} - \underbrace{m_p P_1}_{\text{Loss of producer 1}} \quad (6)$$

$$\frac{dP_2}{dt} = \underbrace{\mu_2 R P_2}_{\text{Uptake of resource}} - \underbrace{m_p P_2}_{\text{Loss of producer 2}} \quad (7)$$

Table 3.2: Table of Parameter Values

Parameter	Value
S_R	0.4 – 1.0
μ_1	3.0
μ_2	2.0
φ_1	0.2
φ_2	0.1
$\delta_N, \delta_1, \delta_2, \delta_C$	0.01, 0.1,0.1, 0.1
ε_1	0.4
ε_2	0.3

Exhaustive list of all parameters used for each simulation run.

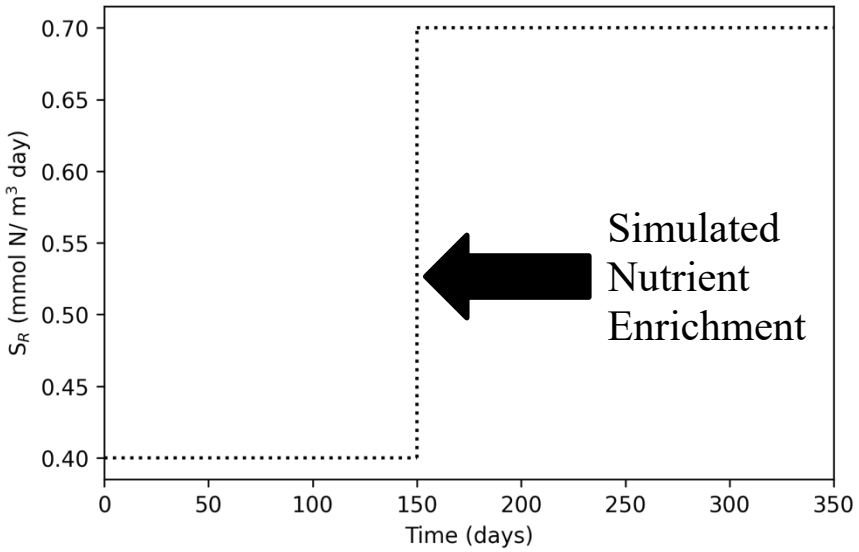

Figure 19: Nutrient Enrichment
Simulated resource enrichment at 150 days in both Model 1A and Model 1B.

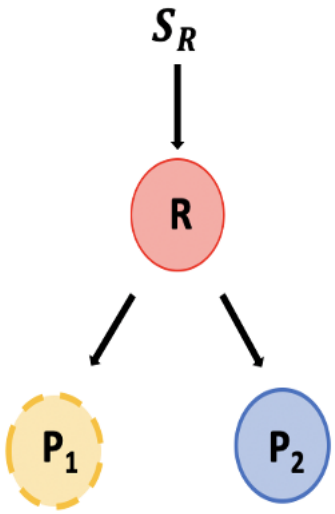

Figure 20: Resource Competition Model
Model 1A-Food-web consisting of a supply rate (S_R), a resource, R, and two producers, P_1 and P_2.

These equations were solved numerically and converged to equilibrium solutions. As a result of the model, P_1 outcompetes P_2 before and after the nutrient enrichment (shown with the black dotted vertical line). This result suggests that the producer better at resource acquisition will outcompete the other producer regardless of the supply rate due to the R^* steady state value of each producer **(Figure 21)**. Previous studies by Tilman, Holt, Armstrong, and Hutchinson give us insight into this resource competition theory and classic outcomes seen when using this food-web structure (Armstrong & McGehee, 1980; Holt et al., 1994; Hutchinson, 1961; Tilman, 1982). However, this model does not take into account the importance of top-down control (Model 1B).

Model 1B consists of two producers competing for a resource, which is supplied at a constant rate. The consumer, which could be a zooplankton or a virus, preys on both groups of producers. The system can be characterized using the following scheme **(Figure 22)** and **Equations 8-9**:

$$\frac{dR}{dt} = \underbrace{S_R}_{\text{Supply rate}} - \underbrace{\mu_1 R P_1 - \mu_2 R P_2}_{\text{Consumption by producers}} \quad (8)$$

$$\frac{dP_1}{dt} = \underbrace{\mu_1 R P_1}_{\text{Uptake of resource}} - \underbrace{\varphi_1 P_1 C}_{\text{Predation}} - \underbrace{\delta_p P_1}_{\text{Background loss}} \quad (9)$$

$$\frac{dP_2}{dt} = \underbrace{\mu_2 R P_2}_{\text{Uptake of resource}} - \underbrace{\varphi_2 P_2 C}_{\text{Predation}} - \underbrace{\delta_p P_2}_{\text{Background loss}} \quad (10)$$

$$\frac{dC}{dt} = \underbrace{\varepsilon_1 \varphi_1 P_1 C + \varepsilon_2 \varphi_2 P_2 C}_{\text{Consumption of Producers}} - \underbrace{\delta_c C}_{\text{Loss of consumer}} \quad (11)$$

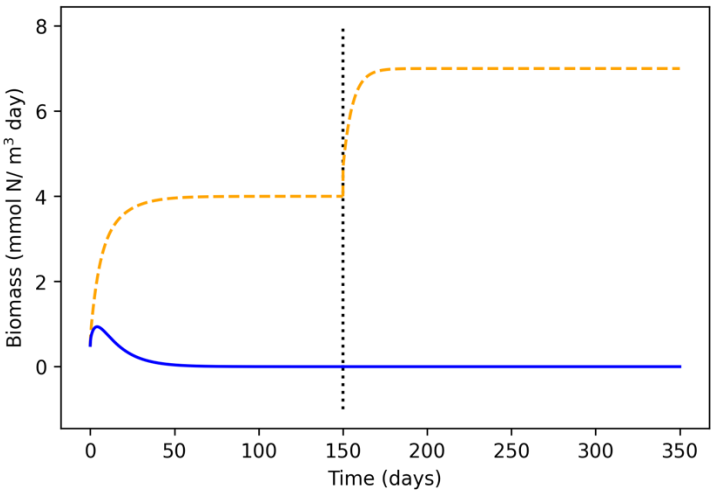

Figure 21: Numerical Solutions for Model 1A
Simulation of the equations for Model 1A (Equation Set 7) solved numerically with resource enrichment at 150 days.

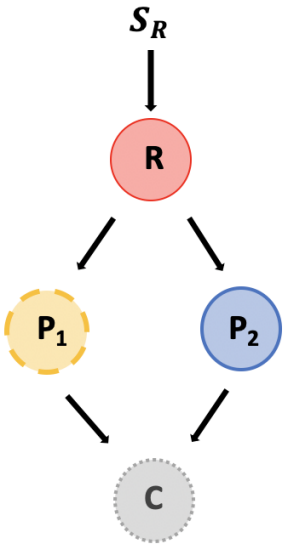

Figure 22: Top-down Control Model
Model 1B - Food-web consisting of a supply rate (S_R), a resource, R, two producers, P_1 and P_2, and a consumer, C.

These equations were solved numerically and converged to equilibrium solutions **(Figure 23).** As a result, P_1 starts to outcompete P_2 before nutrient enrichment. Increases in the resource input (shown as the black dotted vertical line) allows for a transition from the producer better at resource acquisition (P_1) to the producer better at defending against predation (P_2).

These results in **Figure 21** and **Figure 23** imply that the system converges to equilibrium states for fixed supply rates. We calculated all possible equilibrium states (see Appendix). Using our analytical steady-state solutions we can determine how our model will transition from one steady-state to another by increasing our supply rate: **Figure 24**. **Figure 24** shows that at low supply rate (S_R<0.4) we will have steady state solution 1, intermediate supply rates (0.4<S_R<0.65) we will have steady state solution 5, and high supply rates (S_R>0.65) we will have steady state solution 2. This analysis does not account for the potential of sudden influxes of nutrients throughout the year that will affect the populations of producers.

These different model predictions are theoretical scenarios in equilibrium. However, we are unsure of how these equilibrium theories play out in true non-equilibrium conditions. Model 1A and Model 1B have been an important part of our learning process and have given us a good idea of how to build a model that mathematically accounts for non-equilibrium environmental variables such as temperature.

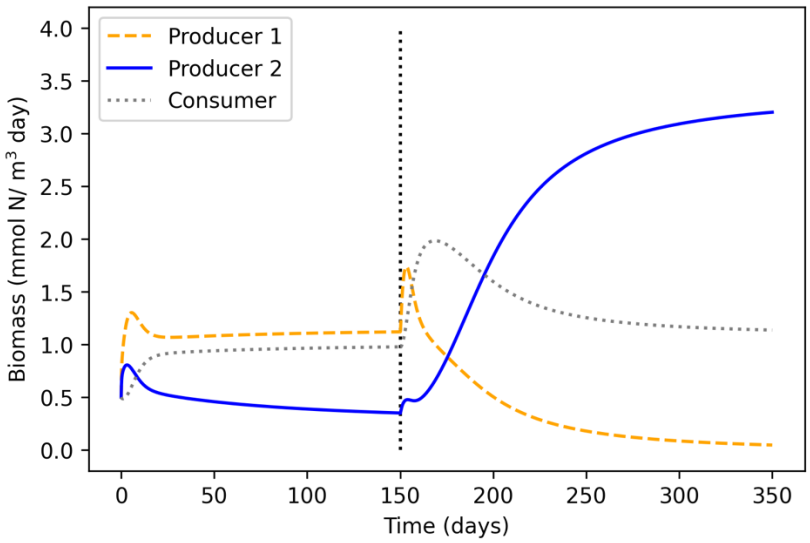

Figure 23: Numerical Solutions for Model 1B
Simulation of the equations for Model 1B (Equation Set 8) solved numerically with nutrient enrichment at 150 days.

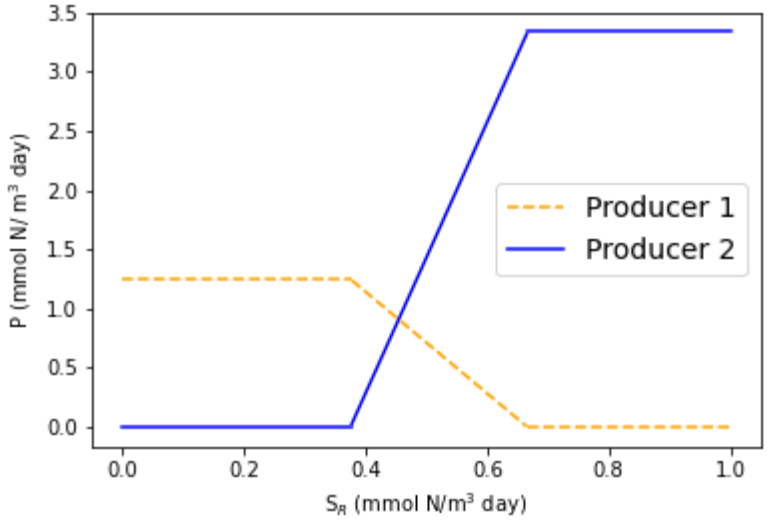

Figure 24: Steady-state Solutions
Analytical steady state solutions for increasing supply rates.

Temperature impacts

A model simulation with a sudden increase in nutrients part of the way through the year is not environmentally realistic. We have solved our model for different nutrient inflows, but we think temperature is likely to be a more variable driver of system structure intra-annually. We therefore altered our model by implementing a linear relationship between resource acquisition parameters and temperature. We also implemented a multiplicative linear relationship between interaction strength of producers and consumers and temperature.

We have solved our model, **Equations 1-4**, numerically at a low temperature (4 degrees Celsius), **Figure 25**. This run of the model shows that at low temperature the producer better at nutrient acquisition will survive better than the producer better at defense against predation. This is what we expected to see because at a low temperature the producer better at resource acquisition will have better fitness due to the consumer group having a low biomass.

Additionally, we have rerun our model, **Equations 1-4**, to numerically solve the equations for high temperature (24 degrees Celsius), **Figure 26**. This run of the model shows that at high nutrients the producer better at nutrient acquisition survives better at first but after a short time the producer that is better at defense against predation becomes the dominant producer group. This is what we expected to see because at a high temperature the producer better at defense against predation will have better fitness due to the consumer group having a high biomass.

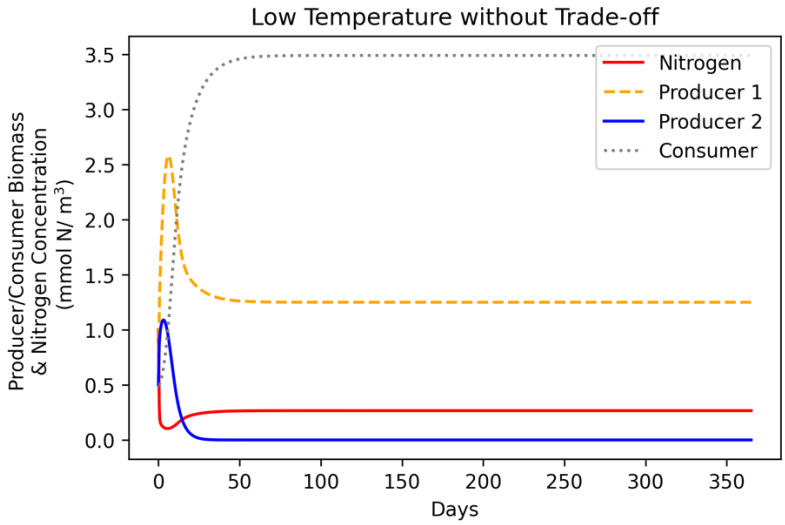

Figure 25: Numerical Simulation at Low Temperature
Numerical simulation of Equations 1-4 at low temperature. The tradeoff would not come into effect because the consumer population would stay low.

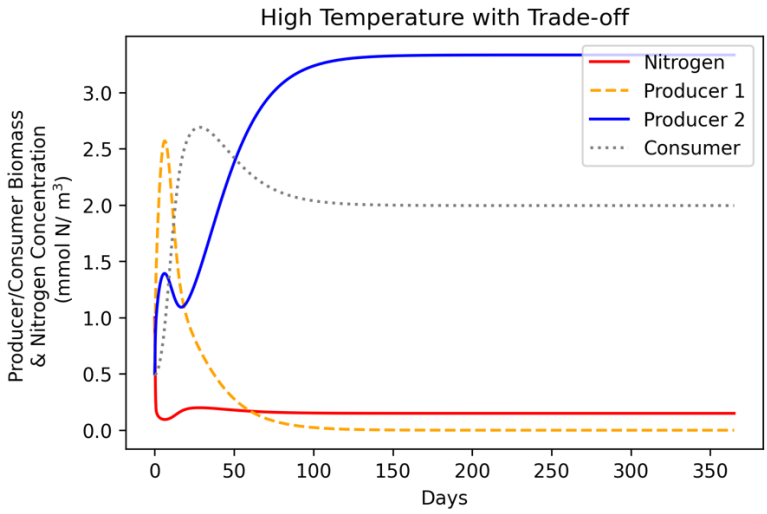

Figure 26: Numerical Simulation at High Temperature
Numerical simulation of Equations 1-4 at high temperature. The tradeoff would come into effect because the consumer population would grow large enough to have an effect of the producer populations.

Temperatures have a relatively consistent cycle throughout the year **(Figure 27).** This cycle can be captured using a sine function, **Equation 12**. We ran this function for three years to show the yearly cycle, **Figure 28**. In this function, we used a T_{min} of 4 degrees Celsius and a T_{max} of 24 degrees Celsius which are the average monthly temperatures at Lake Erie in January and July (Schertzer et al., 1987).

$$T_0 = T_{min} + \left(\frac{T_{max} - T_{min}}{2}\right)\frac{1}{2}\left(\sin\left(\frac{t}{T} * 2\pi - \frac{\pi}{2}\right) + 1\right) \quad (12)$$

We have implemented a multiplicative linear relationship between resource acquisition parameters and temperature. We have also implemented a linear relationship between interaction strength of producers and consumers and temperature. This change in parameters has shown that the producer better at resource acquisition (eukaryotic algae) increases in biomass as the temperature warms but as the consumer biomass grows this allows for the growth of the defense specialist (*Microcystis)*.

Overall, high nutrients and temperature changes allow for the seasonal transition of dominant species from the species good at resource acquisition to the species good at defending against predation. These simulations show the trade-off of resource acquisition and defense occurring between eukaryotic algae (Producer 1) and *Microcystis* (Producer 2) **(Figure 29A).** We compare this to the same model without a trade-off in resource acquisition and defense against predation and do not see a seasonal transition in dominant producer **(Figure**

29B). Finally, we compare these model simulations to the data found from Lake Taihu and find that the model with the trade-off **(Figure 29A)** fits the data qualitatively better as there is a transition between the dominant producers in the later days of the year as seen in the environmental data **(Figure 29C).** Thus, we believe that this model development supports our hypothesis that *Microcystis* ability to protect against predation may be a major reason why it is selected in hyper-eutrophic lakes in the warm late summer months.

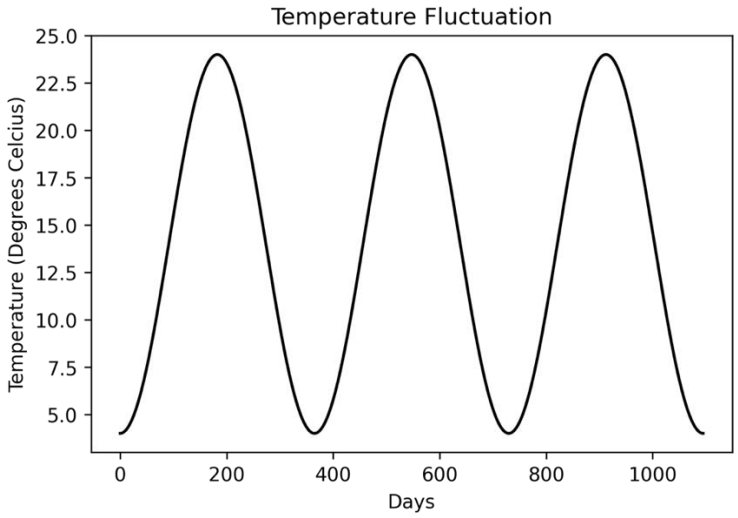

Figure 27: Average Temperature Fluctuation
Simulation of average temperatures (degrees Celsius) from Equation 17.

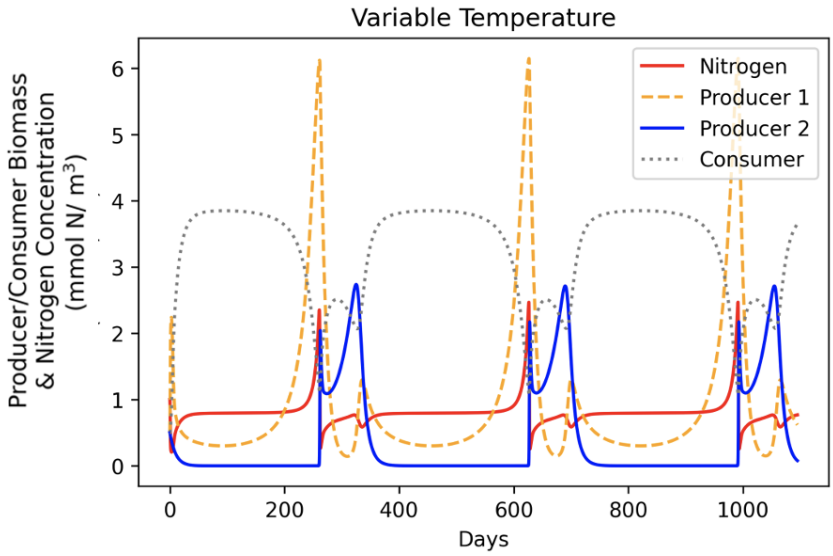

Figure 28: Numerical Simulation at Cycling Temperatures
Nitrogen concentration and biomasses of both producers and consumer when growth rates and consumption rates of producers are impacted by temperature.

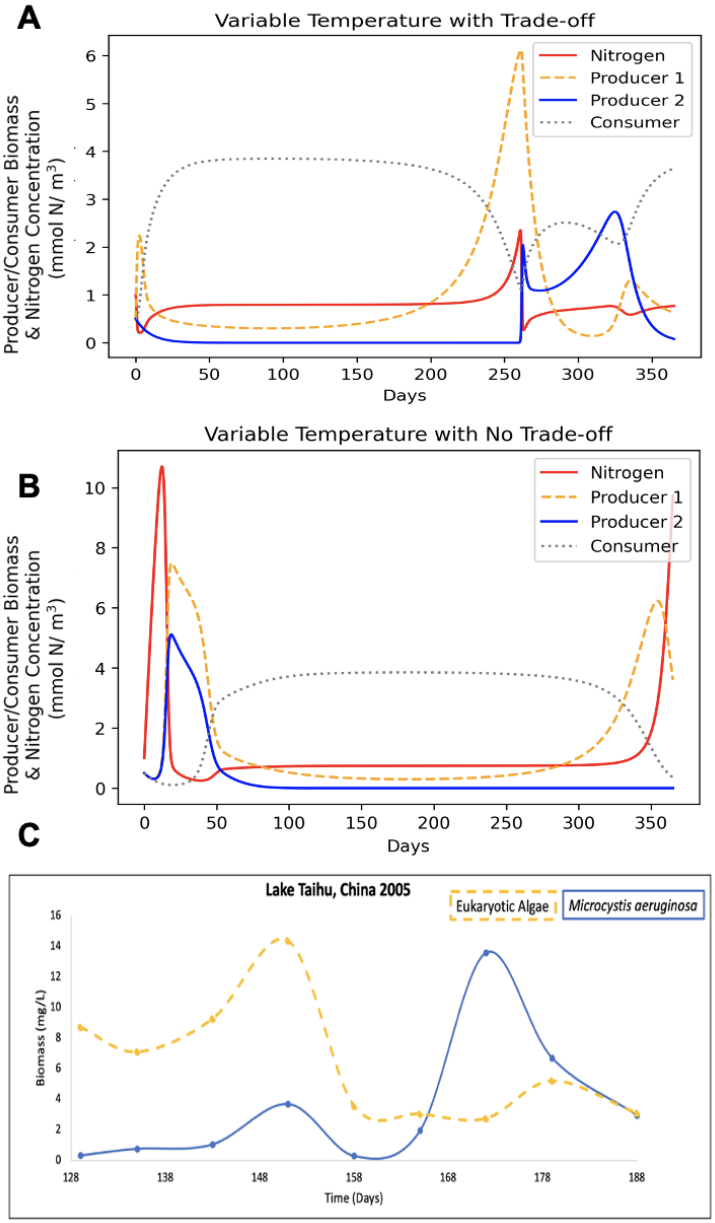

Figure 29: Comparison of Model and Environmental Data
A) Numerically solved equations 1-4, showing a trade-off between the producer better at resource acquisition (Producer 1) and the producer better at defending against predation (Producer 2).
B) Numerically solved equations 1-4 with no trade-off showing no dominant species transition.
C) Data from Lake Taihu showing successional pattern between eukaryotic algae and *Microcystis* (Ke et al., 2008).

CHAPTER FOUR: DISCUSSION

Our data analysis shows that during summer there is a slight draw down of nutrients during an increase in the biomass of both eukaryotic algae and *Microcystis.* As the biomass of phytoplankton increases, we find an increase in the biomass of zooplankton. As the zooplankton biomass increases, we see an increase in the phycocyanin to chlorophyll-a ratio. Thus, supporting the growth of cyanobacteria. Our environmental data analysis led to the hypothesis that shifts in resource inflow causes an increase in contact rates between producers and consumers. Thus, selecting for organisms' better defense against predation, which may be a major reason why *Microcystis aeruginosa* are selected for in hyper-eutrophic lakes. We can test this hypothesis using our mathematical model.

In previous research, *Microcystis* has been implicated as a defense specialist (Lürling, 2021). Lurling determined that increased zooplankton activity select for phytoplankton with defensive traits such as *Microcystis* colony formation (Lürling, 2021). Lurling and Ehrlich et al. proposed that the tradeoff between nutrient acquisition and defense abilities against predation could explain the seasonal shifts in community composition (Ehrlich et al., 2020; Lürling, 2021). However, this idea has not been invoked for *Microcystis* successional dynamics in lake ecosystems. We developed a model to explore the link between a trade-off and the successional pattern occurring in Lake Erie that result in late summer HABs. We have also invoked changes in environmental variables such as

increased nutrient concentrations and temperature fluctuation to determine if this tradeoff and successional pattern hold true in non-equilibrium environmental factors.

Our model development shows that high nutrients and temperature changes allow for the transition of dominant species from the species good at resource acquisition to the species good at defending against predation. Temperature drives an increase in phytoplankton growth and in turn drives an increase in grazing pressure. Thus, leading to a shift in selection pressure from resource acquisition to resisting top-down control. Our simulations show the trade-off of resource acquisition and defense occurring between eukaryotic algae (Producer 1) and *Microcystis* (Producer 2) in both a variable nutrient model and a variable temperature model. Thus, we believe that the environmental data analysis and model development support our hypothesis that enriched resource inflow and temperature selects for defense against predation, which may be a major reason why Microcystis aeruginosa are selected for in hyper-eutrophic lakes.

Limitations of this study include that the study only includes data analysis from one lake that has these seasonal HABs, the model is not in a fully realistic construct and thus, there could be outcomes missed by the lack of non-equilibrium environmental factors included in the model runs. Our model can be amended in future projects to account for other non-equilibrium environmental factors such as irradiance, pH, vertical mixing, etc. The model could also be

amended to test other classic food-web models in these environmentally realistic constructs to determine if these other model theories hold true.

LIST OF REFERENCES

Aguirre, L. E., Ouyang, L., Elfwing, A., Hedblom, M., Wulff, A., & Inganäs, O. (2018). Diatom frustules protect DNA from ultraviolet light. *Scientific Reports*, *8*(1), 1–6. https://doi.org/10.1038/s41598-018-21810-2

Armstrong, R. A., & McGehee, R. (1980). Competitive Exclusion. *The American Naturalist*, *115*, 151–170.

Bhagowati, B., & Ahamad, K. (2019a). A review on lake eutrophication dynamics and recent developments in lake modeling. *Ecohydrology and Hydrobiology*, *19*(1), 155–166. https://doi.org/10.1016/j.ecohyd.2018.03.002

Bhagowati, B., & Ahamad, K. (2019b). A review on lake eutrophication dynamics and recent developments in lake modeling. *Ecohydrology and Hydrobiology*, *19*, 155–166. https://doi.org/10.1016/j.ecohyd.2018.03.002

Brookes, J. D., & Ganf, G. G. (2001). Variations in the buoyancy response of microcystis aeruginosa to nitrogen, phosphorus and light. *Journal of Plankton Research*, *23*(12), 1399–1411. https://doi.org/10.1093/plankt/23.12.1399

Bruggeman, J., & Bolding, K. (2014). A general framework for aquatic biogeochemical models. *Environmental Modelling and Software*, *61*, 249–265. https://doi.org/10.1016/j.envsoft.2014.04.002

Burtner, A., Palladino, D., Kitchens, C., Fyffe, D., Johengen, T., & Stuart, D. (2019). Cooperative Institute for Great Lakes Research, University of Michigan; Fanslow, David; Gossiaux, Duane; National Oceanic and Atmospheric Administration; Great Lakes Environmental Research Laboratory. *Physical, Chemical, and Biological Water Quality Data Collected from a Small Boat in Western Lake Erie, Great Lakes from 2012-05-15 to 2018-10-09 (NCEI Accession 0187718).* https://doi.org/https://www.ncei.noaa.gov/archive/accession/0187718

Campbell, D., Hurry, V., Clarke, A. K., Gustafsson, P., & Öquist, G. (1998). Chlorophyll Fluorescence Analysis of Cyanobacterial Photosynthesis and Acclimation. *Microbiology and Molecular Biology Reviews*, *62*(3), 667–683. https://doi.org/10.1128/mmbr.62.3.667-683.1998

Cao, H. S., Kong, F. X., Luo, L. C., Shi, X. L., Yang, Z., Zhang, X. F., & Tao, Y. (2006). Effects of wind and wind-induced waves on

vertical phytoplankton distribution and surface blooms of microcystis aeruginosa in lake taihu. *Journal of Freshwater Ecology*, *21*(2), 231–238. https://doi.org/10.1080/02705060.2006.9664991

Carmichael, W. W. (1994a). The toxins of cyanobacteria. In *Scientific American* (Vol. 270, pp. 78–86). https://doi.org/10.1038/scientificamerican0194-78

Carmichael, W. W. (1994b). The toxins of cyanobacteria. *Scientific American*, *270*, 78–86. https://doi.org/10.1038/scientificamerican0194-78

Carmichael, W. W. (1997). The Cyanotoxins. In *Advances in Botanical Research* (Vol. 27, Issue C). https://doi.org/10.1016/S0065-2296(08)60282-7

Chunni, Z., Guijun, Y., Boqiang, Q., Wilhelm, S. W., Yu, L., Lihua, H., Zheng, R., Hongwei, Y., & Zhou, Z. (2019). Effects of mixing intensity on colony size and growth of Microcystis aeruginosa. *Annales de Limnologie*, *55*. https://doi.org/10.1051/limn/2019011

Dittmann, E., Neilan, B. A., Erhard, M., Von Döhren, H., & Börner, T. (1997). Insertional mutagenesis of a peptide synthetase gene that is responsible for hepatotoxin production in the cyanobacterium Microcystis aeruginosa PCC 7806. *Molecular Microbiology*, *26*(4), 779–787. https://doi.org/10.1046/j.1365-2958.1997.6131982.x

Ebert, U., Arrayás, M., Temme, N., Sommeijer, B., & Huisman, J. (2001). Critical conditions for phytoplankton blooms. *Bulletin of Mathematical Biology*, *63*, 1095–1124. https://doi.org/10.1006/bulm.2001.0261

Ehrlich, E., Kath, N. J., & Gaedke, U. (2020). The shape of a defense-growth trade-off governs seasonal trait dynamics in natural phytoplankton. *ISME Journal*, *14*(6), 1451–1462. https://doi.org/10.1038/s41396-020-0619-1

EPA, U. S. (2019). Great Lakes National Program Office. *Flat File Data From Zoop Database 4.02_07242019 [Microsoft Excel File]. Retrieved from Https://Cdx.Epa.Gov/*.

EPA, U. S. E. P. A. (2015). *Drinking Water Health Advisory for the Cyanobacterial Microcystin Toxins - 2015*. *June*, 1–75.

Fang, F., Gao, Y., Gan, L., He, X., & Yang, L. (2018). Effects of different initial pH and irradiance levels on cyanobacterial colonies from Lake Taihu, China. *Journal of Applied Phycology*,

30(3), 1777–1793. https://doi.org/10.1007/s10811-018-1394-5
Fernández-Rojas, B., Hernández-Juárez, J., & Pedraza-Chaverri, J. (2014). Nutraceutical properties of phycocyanin. *Journal of Functional Foods*, *11*(C), 375–392. https://doi.org/10.1016/j.jff.2014.10.011
Ger, Kemal A., Hansson, L. A., & Lürling, M. (2014). Understanding cyanobacteria-zooplankton interactions in a more eutrophic world. *Freshwater Biology*, *59*(9), 1783–1798. https://doi.org/10.1111/fwb.12393
Ger, Kemal Ali, Naus-Wiezer, S., De Meester, L., & Lürling, M. (2019). Zooplankton grazing selectivity regulates herbivory and dominance of toxic phytoplankton over multiple prey generations. *Limnology and Oceanography*, *64*(3), 1214–1227. https://doi.org/10.1002/lno.11108
Hansson, L. A., Annadotter, H., Bergman, E., Hamrin, S. F., Jeppesen, E., Kairesalo, T., Luokkanen, E., Nilsson, P. Å., Søndergaard, M., & Strand, J. (1998). Biomanipulation as an application of food-chain theory: Constraints, synthesis, and recommendations for temperate lakes. *Ecosystems*, *1*(6), 558–574. https://doi.org/10.1007/s100219900051
Havens, K. E. (2008). Cyanobacteria blooms: effects on aquatic ecosystems. *Advances in Experimental Medicine and Biology*, *619*, 733–747. https://doi.org/10.1007/978-0-387-75865-7_33
Hellweger, F. L., & Kianirad, E. (2007). Individual-based modeling of phytoplankton: Evaluating approaches for applying the cell quota model. *Journal of Theoretical Biology*, *249*(3), 554–565. https://doi.org/10.1016/j.jtbi.2007.08.020
Ho, J. C., & Michalak, A. M. (2015). Challenges in tracking harmful algal blooms: A synthesis of evidence from Lake Erie. *Journal of Great Lakes Research*, *41*(2), 317–325. https://doi.org/10.1016/j.jglr.2015.01.001
Holt, R. D., Grover, J., & Tilman, D. (1994). Simple rules for interspecific dominance in systems with exploitative and apparent competition. *American Naturalist*, *144*(5), 741–771. https://doi.org/10.1086/285705
Hu, C., & Rzymski, P. (2019). Programmed cell death-like and accompanying release of microcystin in freshwater bloom-forming cyanobacterium microcystis: From identification to ecological

relevance. *Toxins*, *11*(12), 1–19. https://doi.org/10.3390/toxins11120706
Hutchinson, G. E. (1961). The paradox of the plankton. *The American Naturalist*, *95*, 137–145. https://doi.org/10.1017/CBO9781139095075.008
Imai, H., Chang, K. H., Kusaba, M., & Nakano, S. I. (2009). Temperature-dependent dominance of Microcystis (Cyanophyceae) species: M. aeruginosa and M. wesenbergii. *Journal of Plankton Research*, *31*(2), 171–178. https://doi.org/10.1093/plankt/fbn110
Jiang, L., Xia, M., Ludsin, S. A., Rutherford, E. S., Mason, D. M., Marin Jarrin, J., & Pangle, K. L. (2015). Biophysical modeling assessment of the drivers for plankton dynamics in dreissenid-colonized western Lake Erie. *Ecological Modelling*, *308*, 18–33. https://doi.org/10.1016/j.ecolmodel.2015.04.004
Jung, S. W., Kim, B. H., Katano, T., Kong, D. S., & Han, M. S. (2008). Pseudomonas fluorescens HYK0210-SK09 offers species-specific biological control of winter algal blooms caused by freshwater diatom Stephanodiscus hantzschii. *Journal of Applied Microbiology*, *105*(1), 186–195. https://doi.org/10.1111/j.1365-2672.2008.03733.x
Kale, A., & Karthick, B. (2015). The diatoms. *Resonance*, *20*(10), 919–930. https://doi.org/10.1007/s12045-015-0256-6
Ke, Z., Xie, P., & Guo, L. (2008). Controlling factors of spring-summer phytoplankton succession in Lake Taihu (Meiliang Bay, China). *Hydrobiologia*, *607*(1), 41–49. https://doi.org/10.1007/s10750-008-9365-5
Krishnamurthy, T., Szafraniec, L., Hunt, D. F., Shabanowitz, J., Yates, J. R., Hauer, C. R., Carmichael, W. W., Skulberg, O., Codd, G. A., & Missler, S. (1989). Structural characterization of toxic cyclic peptides from blue-green algae by tandem mass spectrometry. *Proceedings of the National Academy of Sciences of the United States of America*, *86*(3), 770–774. https://doi.org/10.1073/pnas.86.3.770
Lampert, W. (1987). Laboratory studies on zooplankton-cyanobacteria interactions. *New Zealand Journal of Marine and Freshwater Research*, *21*(3), 483–490. https://doi.org/10.1080/00288330.1987.9516244

Lindeman, R. L. (1991). The trophic-dynamic aspect of ecology. *Bulletin of Mathematical Biology*, *53*, 167–191. https://doi.org/10.1007/BF02464428

Lürling, M. (2021). Grazing resistance in phytoplankton. *Hydrobiologia*, *848*(1), 237–249. https://doi.org/10.1007/s10750-020-04370-3

Lürling, M., Eshetu, F., Faassen, E. J., Kosten, S., & Huszar, V. L. M. (2013). Comparison of cyanobacterial and green algal growth rates at different temperatures. *Freshwater Biology*, *58*(3), 552–559. https://doi.org/10.1111/j.1365-2427.2012.02866.x

Medarevic, D. P., Losic, D., & Ibric, S. R. (2015). 程鑫 1， 朱泽磊 2 ， 杨桂钟 1 （ 1. *Hemijska Industrija*, *November*, 1–7.

Paerl, H. W., & Huisman, J. (2008). Climate: Blooms like it hot. *Science*, *320*(5872), 57–58. https://doi.org/10.1126/science.1155398

Paerl, H. W., & Paul, V. J. (2012). Climate change: Links to global expansion of harmful cyanobacteria. *Water Research*, *46*(5), 1349–1363. https://doi.org/10.1016/j.watres.2011.08.002

Peng, G., Wilhelm, S. W., Lin, S., & Wang, X. (2018). Response of Microcystis aeruginosa FACHB-905 to different nutrient ratios and changes in phosphorus chemistry. *Journal of Oceanology and Limnology*, *36*(4), 1040–1052. https://doi.org/10.1007/s00343-018-7065-1

Rast, W., & Thornton, J. A. (1996). Trends in eutrophication research and control. *Hydrological Processes*, *10*, 295–313. https://doi.org/10.1002/(SICI)1099-1085(199602)10:2<295::AID-HYP360>3.0.CO;2-F

Reynolds, C. S. (1973). The seasonal periodicity of planktonic diatoms in a shallow eutrophic lake. *Freshwater Biology*, *3*(1), 89–110. https://doi.org/10.1111/j.1365-2427.1973.tb00065.x

Ross, C., Santiago-Vázquez, L., & Paul, V. (2006). Toxin release in response to oxidative stress and programmed cell death in the cyanobacterium Microcystis aeruginosa. *Aquatic Toxicology*, *78*(1), 66–73. https://doi.org/10.1016/j.aquatox.2006.02.007

Rzymski, P., Klimaszyk, P., Jurczak, T., & Poniedziałek, B. (2020). Oxidative Stress, Programmed Cell Death and Microcystin Release in Microcystis aeruginosa in Response to Daphnia

Grazers. *Frontiers in Microbiology*, *11*(June). https://doi.org/10.3389/fmicb.2020.01201
Schertzer, W. M., Saylor, J. H., Boyce, F. M., Robertson, D. G., & Rosa, F. (1987). Seasonal Thermal Cycle of Lake Erie. *Journal of Great Lakes Research*, *13*(4), 468–486. https://doi.org/10.1016/S0380-1330(87)71667-0
Schmidt, J. R., Wilhelm, S. W., & Boyer, G. L. (2014). The fate of microcystins in the environment and challenges for monitoring. *Toxins*, *6*(12), 3354–3387. https://doi.org/10.3390/toxins6123354
Spillane, T. (2016). Diatom frustules as a mechanical defense against predation by geterotrophic dinoflagellates. *WWU Graduate School Collection*, *465*, 1–51.
Tambling, C. J., Minnie, L., Meyer, J., Freeman, E. W., Santymire, R. M., Adendorff, J., & Kerley, G. I. H. (2015). Temporal shifts in activity of prey following large predator reintroductions. *Behavioral Ecology and Sociobiology*.
Tillett, D., Dittmann, E., Erhard, M., Von Döhren, H., Börner, T., & Neilan, B. A. (2000). Structural organization of microcystin biosynthesis in Microcystis aeruginosa PCC7806: An integrated peptide-polyketide synthetase system. *Chemistry and Biology*, *7*(10), 753–764. https://doi.org/10.1016/S1074-5521(00)00021-1
Tilman, D. (1982). Resource Competition and Community Structure. *Princeton University Press, N.J.*
Tilman, D. (2004). A stochastic theory of resource competition, community assembly and invasions. *Proceedings of the National Academy of Sciences of the United States of America*, *101*, 10854–10861.
Urrutia-Cordero, P., Ekvall, M. K., & Hansson, L. A. (2016). Controlling harmful cyanobacteria: Taxa-specific responses of cyanobacteria to grazing by large-bodied Daphnia in a biomanipulation scenario. *PLoS ONE*, *11*(4), 1–14. https://doi.org/10.1371/journal.pone.0153032
Van Dolah, F. M., Lidie, K. B., Monroe, E. A., Bhattacharya, D., Campbell, L., Doucette, G. J., & Kamykowski, D. (2009). The Florida red tide dinoflagellate Karenia brevis: New insights into cellular and molecular processes underlying bloom dynamics. *Harmful Algae*, *8*(4), 562–572. https://doi.org/10.1016/j.hal.2008.11.004

Wilhelm, S. W., Bullerjahn, G. S., & McKay, R. M. L. (2020). The complicated and confusing ecology of microcystis blooms. *MBio*, *11*, 1–5. https://doi.org/10.1128/MBIO.00529-20

Wilson, A. E., Sarnelle, O., & Tillmanns, A. R. (2006). Effects of cyanobacterial toxicity and morphology on the population growth of freshwater zooplankton: Meta-analyses of laboratory experiments. *Limnology and Oceanography*, *51*(4), 1915–1924. https://doi.org/10.4319/lo.2006.51.4.1915

Wu, Z. X., & Song, L. R. (2008). Physiological comparison between colonial and unicellular forms of Microcystis aeruginosa Kütz. (Cyanobacteria). *Phycologia*, *47*(1), 98–104. https://doi.org/10.2216/07-49.1

Xiao, M., Li, M., & Reynolds, C. S. (2018). Colony formation in the cyanobacterium Microcystis. *Biological Reviews*, *93*(3), 1399–1420. https://doi.org/10.1111/brv.12401

Yang, J., Tang, H., Zhang, X., Zhu, X., Huang, Y., & Yang, Z. (2018). High temperature and pH favor Microcystis aeruginosa to outcompete Scenedesmus obliquus. *Environmental Science and Pollution Research*, *25*(5), 4794–4802. https://doi.org/10.1007/s11356-017-0887-0

Zhang, H., Culver, D. A., & Boegman, L. (2008). A two-dimensional ecological model of Lake Erie: Application to estimate dreissenid impacts on large lake plankton populations. *Ecological Modelling*, *214*(2–4), 219–241. https://doi.org/10.1016/j.ecolmodel.2008.02.005

Zhang, M., Shi, X., Yu, Y., & Kong, F. (2011). The acclimative changes in photochemistry after colony formation of the cyanobacteria Microcystis aeruginosa. *Journal of Phycology*, *47*(3), 524–532. https://doi.org/10.1111/j.1529-8817.2011.00987.x

Zheng, J., Zhou, T., & Tao, Y. (2019). Optimized inhibition on Microcystis aeruginosa by combined use of UV-C irradiation and hydrogen peroxide. *IOP Conference Series: Earth and Environmental Science*, *295*(2). https://doi.org/10.1088/1755-1315/295/2/012084

Zhu, W., Sun, Q., Chen, F., & Li, M. (2015). Cellular N:P ratio of Microcystis as an indicator of nutrient limitation—implications and applications. *Environmental Earth Sciences*, *74*(5), 4023–4030.

https://doi.org/10.1007/s12665-015-4707-x
Zuo, J., Chen, L., Shan, K., Hu, L., Song, L., & Gan, N. (2018). Assessment of different mcy genes for detecting the toxic to non-toxic Microcystis ratio in the field by multiplex qPCR. *Journal of Oceanology and Limnology*, *36*(4), 1132–1144. https://doi.org/10.1007/s00343-019-7186-1

APPENDIX

Steady State Solutions

Steady-state solutions are solutions to the system of equations in which the system reaches an equilibrium based on the parameters given in the equations. The system of equations from Equations 1-4 can be set equal to zero and solved for five different possible solution shown below **(Solution 1-Solution 5).**

Solution 1:

Solution 1 contains the Nitrogen group and Producer 1 group as seen in **Figure 19**. This solution set shows the equations for which Nitrogen and Producer 1 groups reach an equilibrium value, **Equation Set 5.**

$$\begin{cases} N \rightarrow \dfrac{\delta_1}{\mu_1} \\ P_1 \rightarrow \dfrac{S_R - \delta_N}{\delta_1} \\ P_2 \rightarrow 0 \\ C \rightarrow 0 \end{cases} \quad (5)$$

This steady-state solution shows that the Nitrogen group equilibrium will be equal to the death rate of Producer 1 divided by the resource affinity of Producer 1. The Producer 1 group will have an equilibrium value equal to the supply rate minus the nitrogen degradation rate and divided by the background death rate of Producer 1. This steady state shows us that only the Producer 1 equilibrium is reliant on the supply rate of Nitrogen.

Figure 19: Solution set 5 diagram - Showing the groups present for this steady state as the resource group and producer 1 group.

Solution 2:

Solution 2 contains the Nitrogen group and Producer 2 group as seen in **Figure 20**. This solution set shows the equations for which Nitrogen and Producer 2 groups reach an equilibrium value, **Equation Set 6**.

$$\begin{cases} N \rightarrow \dfrac{\delta_2}{\mu_2} \\ P_1 \rightarrow 0 \\ P_2 \rightarrow \dfrac{S_R - \delta_N}{\delta_2} \\ C \rightarrow 0 \end{cases} \quad (6)$$

This steady-state solution shows that the Nitrogen group equilibrium will be equal to the death rate of Producer 2 divided by the resource affinity of Producer 2. The Producer 2 group will have an equilibrium value equal to the supply rate minus the nitrogen degradation rate and divided by the background death rate of Producer 2. This steady state shows us that only the Producer 2 equilibrium is reliant on the supply rate of Nitrogen.

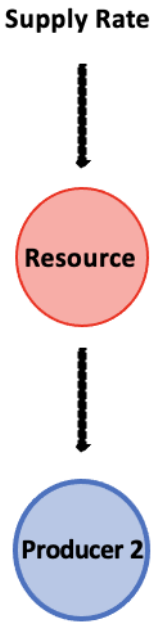

Figure 20: Solution set 6 diagram - Showing the groups present for this steady state as the resource group and producer 2 group.

Solution 3:

Solution 3 contains the Nitrogen group, Producer 1 group, and the Consumer group as seen in **Figure 21**. This solution set shows the equations for which Nitrogen, Producer 1, and Consumer groups reach an equilibrium value, **Equation Set 7**.

$$\begin{cases} N \rightarrow \dfrac{S_R\,\varepsilon_1\,\varphi_1}{\delta_C\,\mu_1 + \delta_N\,\varepsilon_1\,\varphi_1} \\ P_1 \rightarrow \dfrac{\delta_C}{\varepsilon_1\,\varphi_1} \\ P_2 \rightarrow 0 \\ C \rightarrow \dfrac{S_R\,\varepsilon_1\,\mu_1}{\delta_C\,\mu_1 + \delta_N\,\varepsilon_1\,\varphi_1} - \dfrac{\delta_1}{\varphi_1} \end{cases} \quad (7)$$

This steady state shows us that both the Nitrogen group equilibrium and the Consumer group equilibrium are reliant on the supply rate of Nitrogen. However, the equilibrium value for the Producer 1 group is not reliant on supply rate. Thus, as supply rate changes the effect will be on the Nitrogen group and Consumer group but not on the equilibrium vale of the Producer 1 group.

Figure 21: Solution set 4 diagram - Showing the groups present for this steady state as the resource group, producer 1 group, and the consumer group.

Solution 4:

Solution 4 contains the Nitrogen group, Producer 2 group, and the Consumer group as seen in **Figure 22**. This solution set shows the equations for which Nitrogen, Producer 2, and Consumer groups reach an equilibrium value, **Equation Set 8**.

$$\begin{cases} N \to \dfrac{S_R\,\varepsilon_2\,\varphi_2}{\delta_C\,\mu_2 + \delta_N\,\varepsilon_2\,\varphi_2} \\ P_1 \to 0 \\ P_2 \to \dfrac{\delta_C}{\varepsilon_2\,\varphi_2} \\ C \to \dfrac{S_R\,\varepsilon_2\,\mu_2}{\delta_C\,\mu_2 + \delta_N\,\varepsilon_2\,\varphi_2} - \dfrac{\delta_2}{\varphi_2} \end{cases} \quad (8)$$

This steady state shows us that both the Nitrogen group equilibrium and the Consumer group equilibrium are reliant on the supply rate of Nitrogen. However, the equilibrium value for the Producer 2 group is not reliant on supply rate. Thus, as supply rate changes the effect will be on the Nitrogen group and Consumer group but not on the equilibrium vale of the Producer 2 group.

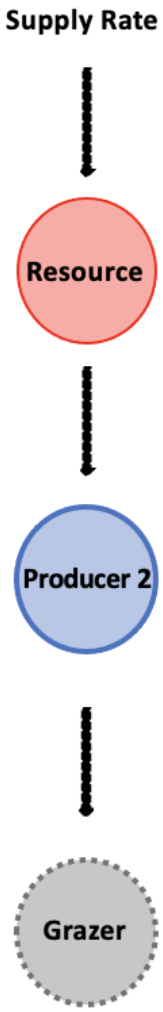

Figure 22: Solution set 8 diagram - Showing the groups present for this steady state as the resource group, producer 2 group, and the consumer group.

Solution 5:

Solution 5 contains all the groups included in our model, **Equations 1-4**, as seen in **Figure 23**. This solution set shows the equations for which Nitrogen, Producer 1, Producer 2, and Consumer groups reach an equilibrium value, **Equation Set 9**.

$$\begin{cases} N \to -\dfrac{\delta_2\,\varphi_1 - \delta_1\,\varphi_2}{\mu_2\,\varphi_1 - \mu_1\,\varphi_2} \\ P_1 \to \dfrac{\delta_2\,\varphi_1(\delta_C\,\mu_2 + \delta_N\,\varepsilon_2\,\varphi_2) - \varphi_2\,(\delta_1\,(\delta_C\,\mu_2 + \delta_N\,\varepsilon_2\,\varphi_2) + S_R\,\varepsilon_2\,(\mu_2\,\varphi_1 - \mu_1\,\varphi_2))}{(\delta_2\,\varphi_1 - \delta_1\,\varphi_2)\,(\varepsilon_1\,\mu_2\,\varphi_1 - \varepsilon_2\,\mu_1\,\varphi_2)} \\ P_2 \to \dfrac{-\delta_2\,\varphi_1(\delta_C\,\mu_1 + \delta_N\,\varepsilon_1\,\varphi_1) + \delta_1\,(\delta_C\,\mu_1 + \delta_N\,\varepsilon_1\,\varphi_1)\,\varphi_2 + S_R\,\varepsilon_1\,\varphi_1\,(\mu_2\,\varphi_1 - \mu_1\,\varphi_2)}{(\delta_2\,\varphi_1 - \delta_1\,\varphi_2)\,(\varepsilon_1\,\mu_2\,\varphi_1 - \varepsilon_2\,\mu_1\,\varphi_2)} \\ C \to \dfrac{\delta_2\,\mu_1 - \delta_1\,\mu_2}{\mu_2\,\varphi_1 - \mu_1\,\varphi_2} \end{cases} \quad (9)$$

This steady state shows us that both the Producer 1 group equilibrium and the Producer 2 group equilibrium are reliant on the supply rate of Nitrogen. However, the equilibrium values for the Nitrogen group and Consumer group are not reliant on supply rate. Thus, as supply rate changes the effect will be on the Producer 1 group and Producer 2 group but not on the equilibrium values of the Nitrogen group or the Consumer group.

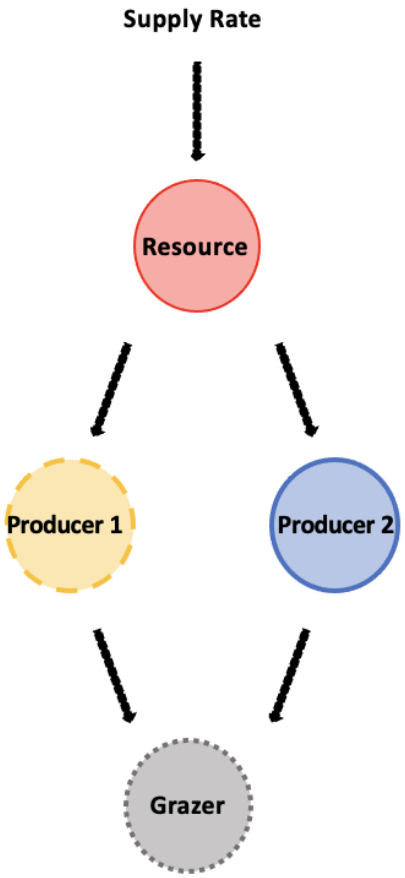

Figure 23: Solution set 9 diagram - Showing the groups present for this steady state as the resource group, producer 1 group, producer 2 group, and the consumer group.

VITA

Kyla Linn Hooker grew up in Tarpon Springs, Florida. She obtained an Associate of Arts degree at The University of West Florida and a Bachelor of Science degree in Mathematics with a concentration in Mathematical Biology at the University of Tennessee. Kyla joined the University of Tennessee/ORNL Graduate School of Genome Science and Technology to pursue a Master of Science degree in Life Science. After graduation, she will be moving to Atlanta, Georgia to teach high school mathematics. She is incredibly grateful for all the support from her husband, family, advisor, and lab mates as she begins her new career.